Modeling the Kinetics of EBV in Primary Carriers and Transplant Recipients

by

Segun M. Akinwumi

A thesis submitted in partial fulfillment of the requirements for the degree of

Doctor of Philosophy

in

Applied Mathematics

Department of Mathematical and Statistical Sciences
University of Alberta

Abstract

Epstein-Barr virus (EBV) is a "kissing disease virus" that has infected more than 95% of the adult human population. It has been associated with diseases such as Acute Infectious Mononucleosis (AIM) and post-transplant lymphoproliferative disorder (PTLD). The kinetics of primary EBV infection has a profound impact on the viral persistence and elements of the kinetic profile have been associated with risk factor for the development of PTLD. In the setting of organ transplantation, optimising immunosuppressive therapy remains difficult because preventing rejection must be balanced against the risk of infection and maligancy. Our knowledge of how immunosuppression affects quantitative levels of EBV-infected cells in transplant recipients is limited. We developed a mathematical model of primary EBV infection based on the biological process of EBV infection of B cells and immune responses to EBV based on the theoretical model of EBV biology known as the germinal center model. We used the model to investigate the impacts of immunosuppression on EBV kinetics in transplant settings by coupling the mathematical model of EBV infection with mathematical models of drugs used to mitigate organ rejection in transplant recipients. The model was able to reproduce patterns of the kinetics of EBV infection observed in clinical data. Our model analysis showed that the rate of EBV infection of naïve B cells, the proliferation rate of infected B cells in the germinal center, and the activation rate of EBV specific cytotoxic lymphocytes (CTL) are key model parameters that strongly influence kinetics of primary EBV infection. The innoculation size of the EBV

affects the peak value of EBV memory B cells and the time to peak. Antiviral treatments of duration 3-6 months have little effect on the EBV-infected memory B celll load, and a perfect antiviral agent applied long-term can clear EBV in this compartment in three years. Antithymocyte globulin appeared to increase both peak and set point in the memory B cell compartment when combined with maintenance immunosuppression alone in contrast to the use of basiliximab. We observed higher peak, longer time to peak, longer time to setpoint, and higher setpoint for infected memory B cells and EBV with antithymocyte globulin combined with maintenance immunosuppression alone compared to the use of basiliximab combined with maintenance immunosuppression. Antiviral treatment given at the time of transplant for period of 3-6 months appeared to reduce peak viral load when combined with either antithymocyte globulin or basiliximab and maintenance immunosuppression.

Keywords: EBV, AIM, PTLD, Mathematical Modeling, Epidemiology, Transplantation, Immunosuppressive drugs, Antithymocyte globulin, Basiliximab, Rituximab, Immunology, Valganciclovir

Preface

The models developed in Chapters 2 and 3 of this thesis were developed by me under the supervision of Dr Li and Dr Preiksaitis. I was responsible for literature reviews, proposing the models, computer simulations, and model analysis. Chapters 2 and 3 of this thesis are manuscripts in preparation for which Michael Akinwumi acknowledges the support of the PIMS IGTC in Mathematical Biology for their scholarship stipend, Dr Michael Li acknoledges support by Natural Sciences and Engineering Research Council of Canada (NSERC) and Canada Foundation for Innovation (CFI).

To my family, extended family, teachers, advisors and friends

"... whatever is true, whatever is noble, whatever is pure, whatever is lovely, whatever is admirable - if anything is excellent or praiseworthy - think about such things." (NIV Bible, Phil. 4.8)

"Whatever your hand finds to do, do it with all your might, for in the realm of the dead, where you are going, there is neither working nor planning nor knowledge nor wisdom." (NIV Bible, Eccl. 9.10)

"When life is a hard game

Don't you blame

It's your chance to

Arise your arm

Let your spirit be brave

Always fight to hold your name

No matter how bad or rough

You never surrender

... "

(The Legend of Bruce Lee. Dir. Moon-ki Lee. China, 2008. Film.)

Acknowledgements

It would almost surely be impossible to successfully pursue a PhD degree without the compact, unwavering support of certain individuals who shaped and continue to shape my history.

Opeyemi Kehinde, thank you for your unwavering belief that God would surely complete all that He starts and all that He started in my life. We have earned this degree together as a family. Mr. Samson Akinwumi and Mrs. Grace Akinwumi, thank you for all your parental guidance and best wishes for my life. This thesis is a testimony of the cumulative effects of your best wishes. My gratitude to siblings, relatives and in-laws who encourage me to pursue my passions.

Dr. Olumide Ogundipe and family, thank you for being a family friend. I value your moral support and encouragements. Dr Joseph Ayeni, thank you for sharing your time and views with me on how to prepare for a life after PhD. Mr. Yemi Nathaniel, I appreciate your financial, parental, and spiritual support. I might still be in Nigeria but for your generous decision to financially support me. Thank you for believing in my life. Chinwendu Ihekweme, thank you for listening to me when I had life challenges in the early days of my studies and for genuinely providing solutions. Dr. Segun Ogundimu, you were like a brother to me during early stages of deciding for the PhD. Your advice indeed yields fruits.

Dr. Adesina Agboola, you exposed me to difficult applied mathematics problem in 2003 during my pre-degree program at the University of Agricul-

ture Abeokuta (UNAAB), Nigeria, renamed Federal University of Agriculture Abeokuta (FUNAAB). Since then my passion for mathematics, especially applied mathematics, has not diminished. Thank you for the mathematical questions that fed my mathematical curiosity. I might not pursue mathematics but for the questions. I had come to UNAAB to study chemical sciences but your math questions helped me to discover my ability and interests.

Dr. Michel Tchuenche, you first exposed me to mathematical biology during my undergraduate days at UNAAB. Thank you for suggesting that I apply to the University of Alberta for a PhD program in Applied Mathematics. You taught me mathematical modeling, supported my PhD application and you frequently cared about my progress in the program, even in your busy career. I have tried to model my own career path after yours. Thank you for demonstrating that "those who study mathematics have got skills that can land them jobs outside academia".

Dr. Michael Li and Dr. Jutta Preiksaitis, thank you for providing the academic environment that is conducive for learning, research and growth. Your support made the journey worthy regardless of the bumps on the road. You both provided an interdisciplinary environment that is invaluable to my success in the program and on my current job. THANK YOU.

There are friends who were part of my life prior to and during the PhD program. I value each minute that you shared in my life journey. I am glad that you chose to contribute to my life.

Table of Contents

List of Tables

List of Figures

Chapter 1

General introduction and outline of the thesis

1.1 Introduction

The Germinal Center Model (GCM) was developed to explain persistent infection by Epstein Barr virus (EBV). Although elementts of the model remain controversial, this model is most consistent with clinical observations and is the most widely accepted model for EBV biology [1, 16–20, 24–27, 30, 52]. EBV is a member of the herpesvirus family and the charactersitic feature of a herpesvirus is the persistent latent infection for the lifetime of its host. Each herpesvirus has a target tissue where it persists and once at the site of persistent infection, it uses optimal gene expression to evade immune responses and persist with minimal effect on the host where it remains for the rest of its hosts life. EBV is B lymphotropic and the virus persists quiescently in resting memory B cells for the lifetime of the host in a non-pathogenic state that is

also invisible to the immune response.

EBV is characterised by an acute viremic stage that resolves into a persistent low-level infectious stage with viral shedding in the saliva that co-exists with persist latency of the virus in memory B cells despite the presence of a potent immune response directed at the virus. Although, periodic higher level of infectious states may occur, in general, the low level of persistence in memory B cells, known as the viral set point, remains remarkably stable for the lifetime of the host [1, 18, 20]. Dynamically, stability is a situation that requires the mechanisms regulating the state to drive it back to the fixed point whenever it is perturbed. The focus of this thesis is to identify measurable clinical parameters that influence the peak and the time to peak of infectious activity, and the virus "setpoint" and the time to "setpoint" during the course of primary EBV infection in both the immunocompetent host and in (solid organ) transplant recipients.

1.2 EBV Biology

1.2.1 Historical perspective, epidemiology and clinical disease associated with EBV infection

In 1964, Epstein-Barr Virus was discovered using electron microscopy to examine a cell line derived from Burkitt's lymphoma tissue [1, 27, 28]. Shortly thereafter, using serologic assays with antigens derived from these cell lines to test patient sera, EBV was found to cause a disease known as acute infectious mononucleosis (AIM) which affected primarily adolescents and young adults in developed countries and was characterized by fever, pharyngitis and lym-

phadenopathy [1, 18]. Although AIM is usually a self-limited infection, it can cause significant morbidity and mortality. On further serologic testing of sera in general populations it was found that EBV infection is almost universal in man. In developing countries, almost all subjects are infected by the age of 5 years and $> 90\%$ of the population is infected by the age of 40 [1, 18, 26, 27]. Infection in childhood is normally asymptomatic and the syndrome known as AIM is seen almost exclusively in adolescence and early adult life. EBV is known to be transmitted by intimate exposure to infected saliva which has resulted in IM being given the moniker of "kissing disease".

1.2.2 The immunocompetent host and primary infection

Studies have suggested that the symptoms associated with IM are immunopathological, that is, caused by an exaggerated immune response to the virus rather than the direct consequences of viral replication [9]. This hypothesis is consistent with the observations from clinical trials of anti-viral agents that inhibit EBV replication. The use of antivirals when a patient presents with AIM symptoms has no significant impact on these symptoms, because at time the patient presents, the immune system has already begun controlling the infection and the symptoms are due to cytokine responses associated with the immune response and not viral replication [7, 8].

There are no non-primate animal models of EBV infection that represent all aspects of EBV biology because it has a very restricted host range; there are also no cell culture models of lytic virus infection [10, 12, 25, 30]. EBV infection is largely asymptomatic and even when studying AIM patients, the

early events of EBV infection have already past by the time symptoms develop and the patient is diagnosed as being acutely infected with EBV [1, 7–9, 18]. Hence, it is extremely difficult to study EBV infection in humans in order to understand its biology. This makes mathematical modeling of the infection along with interventions that might alter the biology of infection extremely useful.

Much of the biology of primary EBV infection occurs in the germinal centers of the tonsils and in lymph nodes that are not amenable to sampling in humans experiencing acute infection. In that setting, we are restricted to measuring EBV DNA in saliva as a surrogate marker of lytic virus replication and EBV DNA in the lymphocytes of peripheral blood as a surrogate marker of the latently infected B cell compartment [22]. There is a limited body of data with respect to viral detection at these two sites in patients already diagnosed with AIM and more recently investigators have studied seronegative college students and young African children not previously infected with EBV and followed them prospectively at regular intervals to obtain data on early events during infection [35,36,150]. This viral data was combined with measurements of the EBV-specific immune response, both serologic and cell-mediated responses. Details of these data are provided below (see section on clinical data related to viral shedding and immune responses during primary EBV infection in Tables2.1 and 3.1). These data provide important clinical information for validating the mathematical models we used.

EBV infection has its major public health impact because it is the prototypical tumor virus and has been associated with a number of malignancies including Burkitt's lymphoma, Hodgkin and non-Hodgkin lymphoma, T/NK

cell lymphoma, and immunodeficiency-associated lymphomas including post-transplant lymphoproliferative disorder (PTLD) [1, 9, 18, 26–28]. Other EBV-associated tumors include nasopharyngeal carcinoma, gastric carcinoma and smooth muscle tumors, the latter occurring largely in subjects who have impaired immune systems [1, 27].

1.2.3 Primary EBV infection in the solid organ transplant setting

A serious complication of the transplantation of solid organs such as kidneys, pancreas, livers, heart, lung and intestinal transplants is an EBV-associated lymphoid malignancy known as post-transplant lymphoproliferative disorder [1, 22, 27, 37]. This often occurs early (i.e. in the first few years after transplant), disproportionately affects children and young adults and is associated with significant morbidity and mortality. Studies of risk factors for PTLD have identified that the patient who is seronegative (i.e. has not been previously exposed to EBV) at the time of transplant and who receives a organ from a donor who is seropositive (i.e. previously exposed) is at significantly increased risk of developing early PTLD [37–39]. Such patients often experience primary EBV infection as the result of EBV transmitted in latently infected donor memory B cells that contaminate the donor organ and from which EBV is reactivated to become lytic and infect recipient B cells. This method of EBV transmission differs from the saliva transmission in immunocompetent subjects.

In a transplant recipient with donor-transmitted EBV infection, primary EBV infection is occurring in the context of a significantly impaired immune system, particularly T cell responses because of the effect of the immuno-

suppressive effects of the drugs the patient is given to prevent organ rejection [40–42]. This is particularly profound early after transplant because of the use of "induction" immunosuppressive agents, most commonly lymphocyte depleting agents such as anti-thymocyte globulin or agents that affects lymphocyte proliferation (i.e. IL2-receptor antagonists such as basiliximab) [42]. These effects are superimposed upon the lifelong effects of maintenance immunosuppression most commonly using drugs such as tacrolimus, mycophenolate mofetil and steroids which are usually tapered to a stable level after the first post-transplant year.

Investigators studying EBV infection after transplant by measuring EBV DNA levels in peripheral blood, primarily and perhaps exclusively in memory B cells, observed that patients who had very high peak viral load measurements in peripheral blood had an increased risk for early PTLD development [22]. This led to prevention programs that involved the monitoring of EBV load in peripheral blood combined with interventions directed at lowering the peak load. Common prevention programs are lowering immunosuppression, use of antiviral drugs or B cell depleting agents when EBV DNA reach specific levels [22]. In addition, some centers give high risk donor EBV seropositive, recipient EBV seronegative anti-viral agents starting at the time of transplant or when viral load is rising to reduce EBV risk [22, 37, 39]. However, it is not clear whether these interventions are effective and their use remains controversial [22]. It is highly unlikely that these interventions will be studied more carefully in randomized clinical trials because of ethical issues, the risk of rejection associated with reducing immunosuppression and the need to use antiviral drugs for other viral complications after transplant. This gives mod-

elling primary EBV infection in a transplant recipient significant potential clinical utility. In the transplant setting, many patients experiencing primary EBV infection early after transplant go on to have markedly elevated EBV viral load in peripheral blood that can persist for many years. It has been suggested that these elevated EBV "set points" may place the patient at increased risk for future PTLD development [22]. In our modeling we therefore studied factors and interventions affecting peak viral load and viral load set points as surrogates of PTLD risk in the transplant population.

1.2.4 The germinal center model

The GCM remains the model that consistently provides a satisfying conceptual framework for understanding the complex behaviours of EBV [1,25,30]. It is built on the simple concept that the virus uses the normal pathways of B cell biology in the lymphoid tissue of Waldeyers ring (tonsils and adenoids) to establish infection, persist and replicate. The virus has evolved to use different gene expression programs - growth program, default program, and latency program - to persist in vivo [1, 28].

The growth program: The target for EBV infection is a resting cell and consequently the virus must initiate latent gene transcription in a quiescent environment. It infects cells through the interaction of the viral glycoproteins gp350/220 with CD21 [43, 44] and gp42/gH/gl with MHC class II on the B cell [45]. The binding of viral particles cause extensive cross-linking of the CD21 signaling complex which provides the signal to begin moving the resting B cells from G0 into the G1 phase of the cell cycle. During this time, the earliest expressed latent protein (EBNA2) is detected. EBNA2 is a tran-

scription factor that activates the promoters essential for production of all the nine latent proteins expressed in the growth program [46]. This transforms infected normal B cells to activated lymphoblasts and begin to proliferate in response to the actions of viral latent proteins [1]. The nine latent proteins of the growth program include six nuclear proteins (EBNAs-Epstein-Barr virus nuclear antigens 1,2,3a,3b,3c and LP) and three membrane proteins (LMPs latent membrane proteins) [1, 28]. Several of the latent proteins have potent growth promoting activity and can act as oncogenes. These include EBNA2, EBNA3a, EBNA3c, and LMP1.

The default program: The growth program drives newly infected B cells to undergo an initial phase of rapid expansion with a division time of approximately 8h for about 3 days [47, 48]. In vivo, these cells become germinal center (GC) cells and switch to the default program which is a more limited form of viral gene expression with EBNA1, LMP1 and LMP2 being the expressed proteins. Cells in the GC latently infected with EBV express the classic GC surface phenotype CD10+, CD77+, CD38+, the functional markers AID and bcl-6 [49], and the correct set of chemokine receptors being CXCR4+, CRCR5+, and CCR7- [1]. The latently EBV-infected germinal center B cells are positive for the proliferation marker Ki67 and undergo multiple rounds of cell division (≥ 20). Despite this, microdissection studies revealed that there are only on average 3-4 latently infected cells per GC. Consequently, the vast majority of latently infected cells produced from the GC mostly die; otherwise, the memory compartment would be overwhelmed [1, 12, 28].

The latency program: EBV in the peripheral blood, is found only in B cells [50] that have the phenotype expected of a latently infected, long-lived,

GC-derived, resting, memory B cell, i.e., classical memory B cells [1, 51–54]. Memory cells latently infected with EBV in the peripheral blood do not express any of the known latent proteins. This led to the conclusion that the site of long-term viral persistence is the memory B cell [1] where it can remain for the lifetime of the host because immunological memory is for life. In the memory compartment, the virus is no longer pathogenic to the host because the genes that drive cellular proliferation and threaten neoplastic disease are turned off.

1.3 Human cytotoxic T lymphocyte responses to Epstein-Barr virus infection

Host immune responses are important in limiting the primary EBV infection and in controlling EBV persistence [55] and the primary and persistent phases of infection are associated with antibody reactivities to lytic and latent EBV antigens [46]. Antibodies to the major virus envelope glycoprotein gp340 can neutralise viral infectivity [56, 57] and to mediate antibody-dependent cellular cytotoxicity against cells in the late phase of virus replication [58]. The frequency of EBV-positive lymphoproliferative disease and clinically apparent virus replicative lesions [60] in T cell-immunocompromised patients strongly suggests an important role for cell-mediated immune responses in the control of EBV. The inhibition of B cell outgrowth by virus-specific cytotoxic T lymphocytes (CTL) is seen only in cultures from virus-immune individuals [55] and it provides the first evidence of long-term CTL surveillance over EBV infection [61].

Primary CTL responses: The prospective study of acute infectious

mononucleosis (AIM) patients offers an opportunity to monitor primary immune response to a viral infection [36, 55]. AIM effectors have been screened directly for EBV antigen and epitope specificity in ex vivo cytotoxicity assays that have detected unequivocally an EBV-specific $CD8^+$ CTL response in AIM that is skewed towards a limited range of epitope peptides, most of which are derived from a subset of latent proteins [62]. $CD8^+$ HLA class I-restricted CTLs to immediate early or early lytic cycle antigens are frequently detectable in the blood of IM patients.

Immunobiology of EBV persistence: Successful infection of a new host depends on the ability of EBV to amplify the load of virus-infected B cells rapidly in the short period prior to the CTL response [55]. The main source of virus involved in this early colonisation of the B cell system is the virions produced from local replicative lesions in the oropharynx. BCRF1, a viral homologue of the cellular IL10 gene [63, 64], is one of the viral genes expressed during the late phase of the lytic cycle. In in-vitro studies, viral IL10 can promote the efficiency of virus-induced transformation through its capacity to augment early B cell proliferation [65, 66] and viral IL10 may serve to impede the local generation of CTL responses either to lytically or to latently infected cells [67].

1.4 Natural killer cells responses to Epstein-Barr virus infection

The depletion of human natural killer (NK) cells enhances AIM symptoms and promotes EBV-associated tumorigenesis [74]. AIM is accompanied by high

EBV titers and massive lymphocytosis caused primarily by EBV-specific $CD8^+$ T cells targeting viral antigens that are involved in lytic infection [68,69]. The counts for the innate lymphocyte natural killer cells have been found to correlate with EBV load in AIM [36,73]. Primary immunodeficiencies that affect NK cells or NK cell recognition of EBV-transformed B cells have been reported to be associated with EBV-positive malignancies and high susceptibility to EBV [70–72,74].

1.5 Previous mathematical models of EBV persistence

1.5.1 Agent-based model of Epstein-Barr virus infection

There is no precise animal model for Epstein-Barr Virus (EBV). Shapiro *et al.* used an agent-based model and computer stimulation of EBV infection to explore the development and resolution of virtual EBV infections and identified parameters capable of inducing clearance, persistent infection, or death [88]. The agent-based simulation of EBV infection was based on the generally accepted features of EBV infection. The model provided a virtual Waldeyers ring of tonsils, adenoids and connecting tissue, as well as virtual cells and virus which interact there. Some of the clinically observed features of EBV infection reproduced by the model include: the development of acute and persistent phases; the suggested peak of acute infection based on literature values; the exponential decay of the infected B-cell population; and the relative sizes of the latently infected vs. lytically replication infected cell pools.

The simulation was performed on a graph that represented the anatomy of Waldeyers ring together with abstract compartments for blood and lymph. Each vertex of the graph was a small volume of tissue and was connected by edges to neighboring vertices. Motion of virtual agents between vertices was controlled according to the type of agent and the type of tissue each vertex represented. Agents only interacted when at the same vertex. Locations on the graph were supplied with populations of virtual virus, B-cells, and T-cells which age, change state, move from one location to the next, and interact according to defined rules. All agents were examined and updated at each time step.

The agent types in the model were virus, naïve B-cells, latently infected B-cells, lytically infected B-cells, naïve T-cells, and two types of activated cytotoxic T lymphocytes (CTLs), one directed against each kind of infected B-cell (CTL latent and CTL lytic). The vertices acted as containers for these agents. In the course of a simulation, there was creation, movement, interaction, aging, and death of agents. A population of naïve B cells and naïve T cells was created to populate the underlying graph. These cells were distributed randomly throughout the entire ring. The numbers of agents created and their lifespans were governed by parameters which were initialised. An infection was initiated by creating a population of virus and distributing these only on the surface of the Waldeyers ring. At each stage of simulations, agents moved to neighboring vertices, interacted, and experienced certain life cycle events triggered by aging, interaction, or motion. The population of naïve B cells in the blood was replenished whenever it dropped.

1.5.2 Mathematical model of age-dependence of Epstein-Barr virus associated infectious mononucleosis

Huynh and Adler proposed a mathematical model for the regulation of EBV infection within a host to address the dependence of infectious mononucleosis on age [10, 89]. The model tracked the number of virus, infected B cell, infected epithelial cell, and $CD8^+$ T- cell responses to the infection. The model suggested that variation in host antibody responses and the complexity of the pre-existing cross-reactive T-cell repertoire, both of which depend on age, may play important roles in the etiology of infectious mononucleosis.

The model assumed that the virus primarily targets two cells types, B cells and epithelial cells. In the model, infection of epithelial cells resulted in cell death and lytic replication with viruses bursting out. The model tracked two types of target cells, B cells and epithelial cells, viruses, two types of specific cytotoxic T cells (CTLs) attacking latently infected B cells (T_2) and lytically infected cells (T_4), respectively, and two types of cross-reacting CTLs against latently (T_{2c}) and lytically (T_{4c})-infected cells. B cells was classified further into four state variables: naïve B cells (B_1), latently infected B cells (B_2), latently infected memory B cells (B_3) and lytically infected B cells or plasma cells (B_4). B_2 and B_3 represented different stages of latency. B_2 were newly infected cells, expressing EBV latent genes and thus recognisable by effector T cells. B_3 represented the next stage of latency with no expression of viral gene and hence no T cell response to these infected memory cells.

The model included two states of epithelial cells: uninfected epithelial cells (E_1), and lytically infected epithelial cells (E_4). Viruses were classified into

virus derived from B cells (V_B) and virus derived from epithelial cells (V_E) and virus produced from one cell type preferentially infected the other. Four state variables for T-cell responses were included to examine the effect of immune responses on the dynamics of infection.

The model consisted of a system of twelve ordinary differential equation as follows.

$$\frac{dB_1}{dt} = d_1(B_0 - B_1) - f(a)\mu_{Eb}V_E B_1 - f(a)\mu_{Bb}V_B B_1, \tag{1.1}$$

$$\frac{dB_2}{dt} = \rho(f(a)\mu_{Eb}V_E B_1 + f(a)\mu_{Bb}V_B B_1) - (d_2 + c)B_2 - k_2 B_2 T_2 - \chi_2 k_2 B_2 T_{2c}, \tag{1.2}$$

$$\frac{dB_3}{dt} = cB_2 + rB_3 - srB_3, \tag{1.3}$$

$$\frac{dB_4}{dt} = rB_3 - d_4 B_4 - k_4 B_4 T_4 - \chi_4 k_4 B_4 T_{4c}, \tag{1.4}$$

$$\frac{dE_1}{dt} = d_e(E_0 - E_1) - h(a)\mu_{Be}V_B E_1 - h(a)\mu_{Ee}V_E E_1, \tag{1.5}$$

$$\frac{dE_4}{dt} = h(a)\mu_{Be}V_B E_1 + h(a)\mu_{Ee}V_E E_1) - (d_e + \gamma)E_4 - k_4 E_4 T_4 - \chi_4 k_4 E_4 T_{4c}, \tag{1.6}$$

$$\frac{dV_B}{dt} = nd_4 B_4 - d_v V_B, \tag{1.7}$$

$$\frac{dV_E}{dt} = n\gamma E_4 - d_v V_E, \tag{1.8}$$

$$\frac{dT_2}{dt} = (1 - \sigma_2)\phi_2 T_N \omega(B_2) + \theta_2 T_2 \omega(B_2) - \delta T_2, \tag{1.9}$$

$$\frac{dT_{2c}}{dt} = \sigma_2 m\phi_2 T_M \omega(B_2) + m\theta_2 T_{2c}\omega(B_2) - m\delta T_2, \tag{1.10}$$

$$\frac{dT_4}{dt} = (1 - \sigma_4)\phi_4 T_N \omega(B_4 + E_4) + \theta_4 T_4 \omega(B_4 + E_4) - \delta T_4, \tag{1.11}$$

$$\frac{dT_{4c}}{dt} = \sigma_4 m\phi_4 T_M \omega(B_4 + E_4) + m\theta_4 T_{4c}\omega(B_4 + E_4) - m\delta T_{4c}. \tag{1.12}$$

The dynamics of B cells satisfied these assumptions:

1. Naïve B cells had an initial population size of B_0 and turnover rate d_1. They were infected by V_B and V_E with rates $f(a)\mu_{Bb}V_B$ and $f(a)\mu_{Eb}V_E$, respectively, where $f(a)$ represents the inhibiting effect of host saliva and antibody responses on the infection of B cells.

2. An infection of a naïve cell B_1 gave rise to one or more latently infected cells B_2 due to the limited proliferation of newly infected cells, where ρ was the proliferation factor. B2 cells died at rate d_2 and were recognised by specific or cross-reactive effector T cells at rate k_2 or $\chi_2 k2$, respectively. They also transformed to latently infected memory state, driven by EBV turning of its gene expression, at rate c.

3. Infected memory cells B_3 experienced homeostatic regulation similar to normal memory B cells. They were not recognised by the immune system and divided at rate r, where one cell became lytic and the other became memory cell. The rate sr represented the death of B_3 due to homeostatic regulation of memory cells, where s was the regulation factor.

4. Lytically infected B cells B_4 resulted from lytic reactivation of memory infected B cells at rate r, burst and released viruses at rate d_4 and were recognised by specific or cross-reactive effector T cells at rate k_4 or $\chi_4 k4$, respectively.

The dynamics of epithelial cells assumed the following:

1. Uninfected epithelial cells had initial population size of E_0 with turnover rate d_e. They were infected by V_B and V_E with rates $h(a)\mu_{Be}V_B$ and $h(a)\mu_{Ee}V_E$, respectively. The enhancement of effect of host saliva and

antibody responses on infection of epithelial cells was represented by h(a).

2. Lytically infected epithelial cells E_4 had a natural death rate of d_e. Death due to virus bursting was at rate γ and these cells were recognised by specific or cross-reactive effector T cells at rate k_4 or $\chi_4 k4$, respectively.

1.5.3 Cyclic pathogenic model of Epstein-Barr virus infection

Hawkins *et al.* developed cyclic pathogen model (CPM) to study interactions between a host and a pathogen, such as EBV, which transits a cycle of antigenically distinct stages [12]. In applying the CPM to the study of EBV, Hawkins *et al.* assumed that persistent infection had reached a stable equilibrium. They also assumed that all the infected stages in the cycle possessed some level of antigenicity and that whether there was an immune response depended on the number of cells at that stage. If it was too high, the immune response would drive the number down to the point where it would just be sufficient to sustain the response. Conversely, if the number was too low, the cells would fail to establish an immune response.

In the cyclic pathogen model (CPM), the pathogen was assumed to transit n distinct stages. This gave rise to 2n populations, the infected stages $S_1 \cdots S_n$ and cognate CTL populations $T_1 \cdots T_n$. These interacted cyclically via the 2n equations, one pair for each value $i = 1, \cdots, n$ and the stage "previous" to stage $i = 1$ was stage $i = n$.

The mathematical model is as follows

$$\frac{dS_i}{dt} = r_{i-1} f_{i-1} S_{i-1} - (a_i + f_i + p_i T_i), \tag{1.13}$$

$$\frac{dT_i}{dt} = (c_i S_i - b) T_i, \tag{1.14}$$

where for each i

1. f_i was the rate at which stage i was lost to become (or produce) stage $i + 1$.

2. r_i was the gain, and was equal to 1 except for the late lytic stage.

3. a_i was the net death rate. This number was negative for a proliferating stage.

4. p_i was the killing efficiency for the CTLs at stage i and encapsulated the likelihood of a CTL finding its target, forming a stable conjugate, and the efficiency of killing.

5. c_i was the net antigenicity of stage i, that is, the efficiency with which stage i maintained CTL activation and provoked CTL proliferation.

6. b was the rate of decay of the CTL response in the absence of antigen.

1.5.4 Our contribution to mathematical models of EBV infection

Shapiro *et al.* eventually developed a computer simulation of EBV pathogenesis after dissatisfaction with attempts to model EBV infection using differential equations and difference equations [88]. One big drawback of using

agent-based models is that there is no satisfying mathematical theory that allows model results to be reproducible. The model did not consider the growth program, default program and latent program of EBV separately. There was no attempt to model the innate immune system and ntibody activity was only implicitly modeled in virus life-span. We developed a mathematical model that is based on generally accepted model of EBV infection and that overcomes most of the challenges faced by the agent-based simulation model of EBV pathogenesis. The model is a system deterministic differential equations and it was simulated based on the biologically feasible parameters used by Shapiro *et al.*

We improved the Huynh-Adler model [10, 89] by adding a separate compartment for infections EBV virions, and splitting the latently infected B cells (B_2) into two B cells types: B cells expressing the growth program; and B cells expressing the default program. This approach better approximated the actual pathogenesis of EBV and it would allow specific investigations of the roles played by these cell types in EBV infection. Our focus was not on age-specific roles of EBV and hence we did not consider the roles of cross-reacting CTL responses. There are open questions on the roles of epithelial cells in EBV infection and due to reasons discussed in chapter 4 of this thesis, we did not consider it in our work. We considered three CTL responses to infected B cells expressing the growth program, the default program and the lytic program.

We developed a 6-stage model similar to Hawkins *et al.* 's model by including a compartment each for EBV and naïve B cells. We did not differentiate between immediate early lytic, early lytic and late lytic stages. We assumed that the transcription and translation of the lytic proteins occur on a very

fats time scale. Similar to Hawkins *et al.* 's, we had separate compartments for infected proliferating B cells, infected germinal cells and lytically infected B cells. We also assumed that there was an immune response to each infected compartment except for the memory stage.

1.6 Thesis Outline

The focus of this thesis is to identify measurable clinical parameters that influence the homeostatic phase in primary EBV infection in immunocompetent subjects and in (solid organ) transplant recipients. We addressed two research questions in this thesis:

1. What are the implications of kinetics of primary EBV infection for EBV persistence and disease management?

2. What are the impacts of immunosuppressive therapy and antiviral treatment on EBV kinetics in transplantation?

In chapter 2, we address the first research question. We developed a mathematical model that is based on the Germinal Center Model (GCM). We derived the basic reproduction number for the model and its value is consistent with EBV persistence, thus supporting the GCM framework for EBV infection dynamics. We identified key parameters that influence the kinetics of infected memory B cells together with impacts of short-term and long-term antiviral treatments, and innoculation size on the kinetics of infected memory B cells

In chapter 3 we focus on the second research question. We coupled the mathematical model of EBV discussed in chapter 2 with mathematical models

for maintenance immunosuppression treatments, induction treatments, antiviral treatments and rituximab treatments in (solid organ) transplant recipients. We investigated how maintenance immunosuppressive drugs, antithymocyte globulin, basiliximab, antiviral treatment (using valganciclovir), rituximab, and innoculum impact the peak and the time to peak of EBV infectious activity, and the virus setpoint and the time to setpoint during the course of primary EBV infection in transplant recipients. We summarised our findings in chapter 4 with a discussion of limitations and possible ways to extend this work. We have the MATLAB files used for the analysis in the appendix.

Chapter 2

Modeling the kinetics of primary EBV infection in the immunocompetent host with implications for viral persistence and disease management

2.1 Introduction

EBV infection is asymptomatic in over 95% of the adult human population [75–77, 83, 86], and it is associated with life-threatening complications in solid organ transplants [75, 77, 101]. Primary EBV infection can result in acute infectious mononucleosis (AIM) with a prevalence between 20% and 50% [86]. AIM is a lymphoproliferative disease that may persist for weeks or months,

and it may permanently damage the immune system [86]. Primary EBV infection is also an important risk factor in several B-cell lymphomas, including post-transplant lymphoproliferative disorder (PTLD) [80–82, 101].

Understanding the kinetics of primary EBV infection of B cells and the role of EBV-specific cytotoxic lymphocytes (CTL) immune responses is key to understand the viral dynamics of EBV during acute AIM and the long-term viral oersistence. It will also provide insights into the development of the PTLD and better management of the EBV infection among solid organ transplant patients. To quantify the kinetics of primary EBV infection, we developed mathematical models of EBV infection and CTL responses based on the best biomedical knowledge of EBV pathogenesis as formulated in the Germinal Center Model (GCM), first proposed by Thorley-Lawson and his collaborators [79, 81, 87]. Our primary objective was to quantify several important characteristics of kinetics of primary EBV infection and compare our model predictions to clinical data. The important characteristics we studied include the peak value of EBV viral load, time it takes to reach the peak, the role of EBV-specific responses and NK cells, and the impact of innoculation size of EBV. Using sensitivity analysis we were able to identify key model parameters that strongly influence these characteristics. Estimation of the basic reproduction number of the EBV primary infection using our model allowed us to investigate long-term persistence of EBV. We also incorporated into our model both short-term and long-term treatmentsusing the current antiviral agaents to study viral management and EBV clearance. Earlier modeling studies of the dynamics of EBV infection primarily focused on factors that lead to EBV persistence. Shapiro *et al.* [88] proposed an agent-based

model of EBV infection to identify parameters that contribute to EBV persistence. Huynh and Adler [89] proposed a deterministic mathematical model of EBV infection and studied the role of epithelial cells in EBV persistence. Adapting a general multistage model of pathogen infection of Delgado-Eckert and Shapiro [109] to EBV infection, Hawkins *et al.* [90] was able to show the model posseses a unique positive equilibrium and predicts long-term persistence of EBV, which further validated the Germinal Center Model (GCM) of EBV infection. In comparison, our modeling study focus on quantitative analysis of the kinetics of primary EBV infection and characteristics that have significant clinical implications. Our model and results laid the foundationfor further modelingstudies of management of EBV infection among solid organ transplant using maintenance therapies and antiviral treatments.

2.2 The Germinal Center Model of EBV pathogenesis

Thorley-Lawson et al. [79,81,87] proposed a Germinal Center Model (GCM) for the pathogenesis of EBV infection. The idea that EBV exploits the normal pathway of B-cell differentiation forms the backbone of GCM [78–82, 86, 87]. The sequence of events in EBV infection cycle begins with acquiring EBV virons from saliva exchange with an infected individual and the EBV infection of naïve B cells occurs in the layer below the epithelial cells in the *TONSILAR CRYPTS* to infect a portion of the underlying pool of naïve B cells. Early differentiation of NK cells can restrict lytic EBV infection [102]. The virus can then express a set of nine genes, which constitute its growth program,

and transform the infected B cells into proliferating B blasts. EBV then expresses a restricted set of three genes, that constitute its default program, to transform the B blasts into default B blasts. The default B blasts undergo rapid proliferation in the germinal center while under active CTL response. Two viral proteins resulting from the default program provide signals to rescue some of the default B blasts into the memory compartment where they can become persistently infected memory B cells. Infected memory B cells occasionally reactivate to become cells that undergo lytic replication. These lytic cells can then release infectious EBV particles that can infect naïve B cells. Host immune responses to EBV include early differentiation of NK cells that can restrict EBV infection [102], and EBV-specific cytotoxic T lymphocyte responses to infected B cells at different stages. The GCM is graphically depicted in Figure 2.1. Several modeling studies have validated that GCM can explain long-term persistence of EBV [89, 90].

2.3 A Mathematical Model of Primary EBV Infection

Our mathematical model of primary EBV infection is based on GCM and contains all the key stages of EBV infection cycle described in GCM (Figure 2.1). The model has nine interacting agents: free EBV virons, naïve B cells, infected proliferating B blasts, infected default B blasts, infected memory B cells, lytically infected B cells, and three different cytotoxic T lymphocytes (CTLs) specific to the infected proliferating B blasts, default B blasts and lytic B cells:

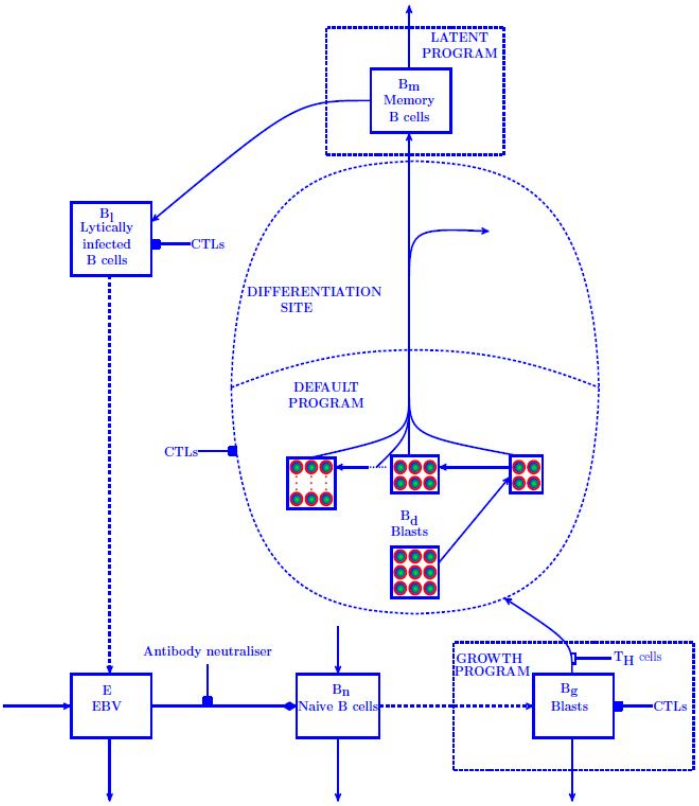

Fig 2.1. A graphic representation of the germinal center model.

- E - Epstein-Barr Virus;
- B_n naïve B cells;
- B_g - infected B cells expressing the growth program;
- B_d - infected B cells expressing the default program;
- B_m infected memory B cells;
- B_l - lytic infected B cells;
- T_g - CTLs specific to infected B_g cells;

- T_d - CTLs specific to infected B_d;
- T_l - CTLs specific to B_l cells.

2.3.1 Derivation of the mathematical model

We assume that EBV is produced at some rate δ_l per lytic infected B cell B_l with burst size n, and that the turnover rate of EBV particles is δ_e. The equation for the dynamics of EBV particle is given by

$$\frac{dE}{dt} = n\delta_l B_l - \delta_e E.$$

In Figure 2.1, we use the input arrow from the environment into the EBV compartment E to represent a source of EBV infection through exchange of infected saliva. We do not consider this in our work.

EBV particle infects naïve B cells at an effective rate μ_e. We assume that naïve B cells are produced at a constant rate λ_n and that the death rate of naïve B cells is δ_n. The equation for naïve B cell dynamics is given by

$$\frac{dB_n}{dt} = \lambda_n - \mu_e E B_n - \delta_n B_n.$$

The infected naïve B cells, $\mu_e E B_n$, transform into proliferating infected B cells B_g by expressing the growth program of EBV [78–82, 87]. The transformation can be modulated by early differentiation of NK cells [102] and we use β to represent this effect. These infected B cells B_g can die at a constant rate δ_g, become rescued into the germinal center at some constant rate ω_g, and proliferate at a rate r_g. The CTL response to the B cells expressing the growth program is modeled by $\delta_1 T_g B_g$. The dynamics of the B_g cells is given

by

$$\frac{dB_g}{dt} = (1-\beta)\mu_e E B_n + (r_g - \omega_g - \delta_g)B_g - \delta_1 T_g B_g.$$

We assume that a fraction $\omega_g B_g$ of the infected B cells transit to the germinal center to express the default program of EBV. In the germinal center, infected B cells B_d proliferate at a rate r_d, die at a rate δ_d, and undergo CTL-induced apoptosis at a rate $\delta_2 T_d B_d$. A fraction w_d of B_d is rescued into the memory compartment. The dynamics of the B_d cells is given by

$$\frac{dB_d}{dt} = \omega_g B_g + (r_d - \delta_d - \omega_d)B_d - \delta_2 T_d B_d.$$

The default program of EBV provides signals which can rescue the infected germinal B cells into the memory B cell compartment [79–82, 87] at a rate $\omega_d B_d$. These infected memory B cells proliferate at a rate r_m, become lytic infected B cells at a rate ω_m and die at a rate δ_m. We assume that there is no CTL response to the memory compartment [88–90] since memory B cells do not display EBV proteins that can stimulate immune response. The equation governing the memory compartment is

$$\frac{dB_m}{dt} = \omega_d B_d + (r_m - \omega_m - \delta_m)B_m.$$

Infected memory B cells can reactivate to become lytically infected B cells B_l at a rate ω_m and these lytic B cells die at a rate δ_l. We use $\delta_3 T_l B_l$ to model the CTL response to the lytic B cells. The dynamics of the lytic B cells is governed by

$$\frac{dB_l}{dt} = \omega_m B_m - \delta_l B_l - \delta_3 T_l B_l.$$

To model the dynamics of CTLs, we assume that the proliferation of T_g that are specific to B_g is described by $r_1 T_g B_g$, and that the turn-out rate is given by d_1. The dynamics of CTLs T_g is given by

$$\frac{dT_g}{dt} = r_1 T_g B_g - d_1 T_g.$$

Equations that govern CTLs T_d and T_l that are specific to B_d and B_l, respectively, can be derived similarly, with respective proliferation rates r_2 and r_3, and turn-over rates d_2 and d_3.

The EBV infection dynamics is modeled by the following system of differential equations 2.1–2.9:

$$\frac{dE}{dt} = n\delta_l B_l - \delta_e E, \tag{2.1}$$
$$\frac{dB_n}{dt} = \lambda_n - \mu_e E B_n - \delta_n B_n, \tag{2.2}$$
$$\frac{dB_g}{dt} = (1-\beta)\mu_e E B_n + (r_g - \omega_g - \delta_g) B_g - \delta_1 T_g B_g, \tag{2.3}$$
$$\frac{dB_d}{dt} = \omega_g B_g + (r_d - \delta_d - \omega_d) B_d - \delta_2 T_d B_d, \tag{2.4}$$
$$\frac{dB_m}{dt} = \omega_d B_d + (r_m - \omega_m - \delta_m) B_m, \tag{2.5}$$
$$\frac{dB_l}{dt} = \omega_m B_m - \delta_l B_l - \delta_3 T_l B_l, \tag{2.6}$$
$$\frac{dT_g}{dt} = r_1 T_g B_g - d_1 T_g, \tag{2.7}$$
$$\frac{dT_d}{dt} = r_2 T_d B_d - d_2 T_d, \tag{2.8}$$
$$\frac{dT_l}{dt} = r_3 T_l B_l - d_3 T_l. \tag{2.9}$$

2.3.2 Model parameters

The model parameters are given in Table 2.1, together with their biological interpretations. The numerical values of parameters in the list were obtained from the research literature as detailed in the corresponding references. Infected B cells in the germinal center divide approximately every 6 to 12h and they undergo approximately three rounds of cell division before they die or leave [108]. We used this information to assume that an infected B cell divides every 9h (the mean of 6h to 12h) and then accordingly estimated the proliferation rate of infected GC B cells. We assumed a value for the effect of natural killer (NK) cells of the interaction between EBV and naïve B cells [102].

Our model is the first to explicitly consider all the known stages of EBV infections as outlined in [79, 81, 82, 87, 98]. In particular, we considered all the latent infection stages of B cells since they play significant roles during the primary EBV infection and are essential for our quantitative analysis of the kinetics of the viral dynamics.

Table 2.1. Baseline parameters used in simulations of equations 2.1–2.9. The parameters are measured in per week except for n and β that are dimensionless.

Parameter	Description	Value	Reference
n	viral burst size	1.00×10^5	[88, 89]
δ_l	Death rate of lytically infected cell due to viral burst	2.32×10^{-4}	[88, 89]

δ_e	Death rate of EBV	2.33	[88]
λ_n	Production rate of naïve B cells	5.04×10^5	[88, 89]
β	NK cells effects on EBV infection	0.80	[1]
μ_e	EBV infection rate per B cell virus	3.3×10^{-8}	[89]
δ_n	Death rate of naïve B cells	1.68	[88]
r_g	Proliferation rate of infected B cells expressing the growth program	37.8	[88, 89]
ω_g	Transit rate from growth compartment to default compartment	4.90	[89]

[1] Assumption.

δ_g	Death rate of infected B cells expressing the growth program	0.88	[88, 89]
δ_1	Rate at which CTL kills infected B cells expressing the growth program	3.83×10^{-4}	[89]
r_d	Proliferation rate of infected B cells expressing the default program	38.81	[108]
ω_d	Transit rate from default compartment to memory compartment	10.08	[89, 108]
δ_d	Death rate of infected germinal B cells expressing the default program	10.08	[89, 108]

δ_2	Rate at which CTL kills infected B cells expressing the default program	3.83×10^{-4}	[89]
r_m	Proliferation rate of infected memory B cells	0.00	[88, 89]
ω_m	Reactivation rate of infected memory B cells into lytically infected B cells	0.84	[88, 89]
δ_m	Death rate of infected memory B cells	0.00	[79, 81, 87]
δ_3	Rate at which CTL kills lytically infected B cells	7.66×10^{-4}	[88, 89]

r_1	Rate of CTL activation against infected B cells expressing the growth program	1.40×10^{-3}	[88, 89]
r_2	Rate of CTL activation against infected B cells expressing the default program	2.10×10^{-3}	[88–90]
r_3	Rate of CTL activation against lytically infected B cells	4.90×10^{-3}	[88, 89]
d_1	Death rate of CTLs responding to the growth compartment	6.46×10^{-2}	[88, 90]
d_2	Death rate of CTLs responding to the default compartment	6.46×10^{-2}	[88, 90]

d_3	Death rate of CTLs responding to the lytic compartment	6.46×10^{-2}	[88, 90]

2.3.3 LHS-PRCC methodology

Sensitivity analysis is used to identify key model parameters that have strong influence on the kinetics of EBV infection dynamics. Latin hypercube sampling (LHS) is an efficient Monte Carlo sampling technique that partitions each parameter's range into N equal intervals and randomly draws only one sample from each interval based one a specified distribution [84, 103, 104].

Partial rank correlation coefficient (PRCC) is a measure of nonlinear, monotonic relationship between a pair of variables after adjusting for linear effects of all parameters of no interest [84, 104]. The Pearson's correlation coefficient

$$\rho_{X,Y} = \frac{\sum_{i=1}^{n} (x_i - \bar{x})(y_i - \bar{y})}{\sqrt{\sum_{i=1}^{n} (x_i - \bar{x})^2 \sum_{i=1}^{n} (y_i - \bar{y})^2}},$$

quantifies linear relationship between X and Y where

$$\{(x_i, y_i) : x_i \in X \text{ and } y_i \in Y\}$$

is the set of paired samples.

Let

$$\hat{X}_j = b_0 + \sum_{\substack{i=1 \\ i \neq j}}^{k} b_i X_i \text{ and } \hat{Y} = \beta_0 + \sum_{\substack{i=1 \\ i \neq j}}^{k} \beta_i X_i.$$

PRCC computes the correlation between the residuals $(X_j - \hat{X}_j)$ and $(Y_j - \hat{Y})$ where X_j is the rank transformed j$^{\text{th}}$ sample of the input parameter and Y is the rank transformed response variable [84, 104]. If there is more than one input variable, partial correlation provides a measure of the strength and the direction of trends between output and input variables while controlling for the linear effects of the other input variables [84, 104].

2.3.4 Identifying influential model parameters

Characteristics of the kinetics of primary EBV infection that have clinical significance are peak value, peak time and set point of the EBV viral load. The measure for the EBV viral load is the number of latently infected B cells in the memory compartments, since this can be clinically measured from patients. In the following sequence (see [84,104]), we applied the LHS-PRCC methodology above to the model 3.1–3.9 to identify parameters that significantly influence different characteristics of EBV infection kinetics.

1. Sampling: We applied LHS to sample from the space of the parameters in equations 3.1–3.9.

2. Response: We simulated equations 3.1–3.9 with the samples and estimated outputs of interest.

3. Ranking: We ranked both parameter samples and response values and replaced their original values with their ranks.

4. Correlation effect: We calculated PRCC for each input parameter.

We used the parameters in Table 2.1 as baseline values for the analysis. We used LHS-PRCC-based sensitivity analysis techniques to vary some model parameters around their baseline values, drawing 2000 samples of each parameter from an interval centered at the baseline with interval width of 100. This range was chosen to ensure a biologically feasible parameter set (see [90] for details). We considered all model parameters for sensitivity studies and we used $\pm$ 0.4 as threshold partial correlation coefficient (PRCC) or the vulnerability of a parameter to intervention as a criterion for streamlining the parameter list.

2.3.5 Antiviral treatments

Acyclovir and its improved form Valganciclovir are among the antiviral drugs that have shown *in vitro* activity against EBV. During reactivation phase of latently infected memory B cells, EBV replicates using the viral DNA polymerase, which is inhibited by acyclovir. By blocking the replication of EBV in lytic memory B cells, the action of acyclovir directly impacts the burst size n of EBV particles from a lytic memory B cell.

Several clinical studies showed that these drugs can completely inhibit EBV shedding in the saliva but were unable to significantly reduce EBV load in the blood during short-term treatment of length less than 28 days. A clinical study of long-term treatment (12 months) of EBV infected individuals using valganciclovir showed a significant reduction of EBV viral load in the blood [95, 105]. It was suggested that long-term treatment of valganciclovir has the potential to clear EBV infection if no reinfection occurs.

We studied the effects of antiviral treatments using our model by con-

sidering different levels of viral burst size n in equation 3.1 and for different lengths of treatment course. We have also considered the effects of starting the antiviral treatmentat different time point during the course of infection.

2.4 Results

We present simulated profiles of viral loads and infected target cells based on equations 3.1–3.9. We established a linear association between CTL response to lytic B cells and proliferation rate of infected memory B cells or decline rates of infected memory B cells. We present correlates for peak value, time to peak, set-point and time to set-point for infected B cells. We discuss results of simulated short-term and long-term treatment effects on clearance of infected memory B cells. The simulated impact of innoculum size on some of model compartments are discussed.

Results are reported using simulation outputs for compartments of the memory B cells and free EBV, although we observed similar results for other compartments. Free Epstein-Barr virus is used as a surveillance tool for strategies used for the prevention of EBV-associated complications [76]. Infected memory B cells compartment is the site of latent EBV infection and these cells correlate with viral load in cellular blood compartment [76, 79, 81, 86–89, 105, 106].

2.4.1 Profile of viral load

Our model simulations were able to reproduce characteristic three-phase profile of primary EBV infection observed in clinical data [86–88]. Clinical studies of primary EBV infection have shown that EBV viral load peaks be-

tween five to six weeks post-infection [86, 105, 106], and followed by a rapid decline for about one week [86, 106, 107]. The rapid decline is followed by a homeostatic phase where the virus persists possibly throughout the host lifetime [79, 81, 82, 86–88]. Using the parameter values in Table 2.1, our model simulations showed a viral peak time about 5 weeks post infection. As shown in Figure 2.2, our model simulations were able to capture these key features quantitatively.

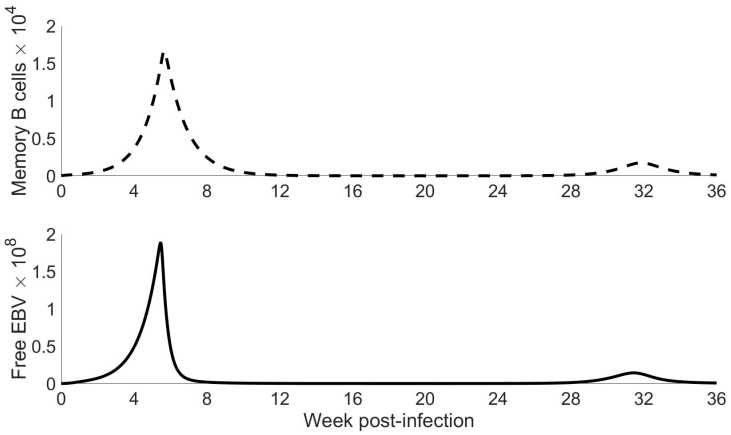

Fig 2.2. Model replicates clinical observations of general profile of EBV infection: steady expansion, followed by rapid decline and then homeostasis. Our model simulations showed a peak time at about 5 weeks post infection in numbers of both free EBV and latently infected memory B cells, a rapid decline from peak for about one week, and long-term persistent EBV infection.

2.4.2 Model basic reproduction number

The basic reproduction number of a disease dynamics is a key parameter whose value determines the outcome of an infection. For model 3.1–3.9, the basic reproduction number R_0 is the average number of secondary cases of EBV infection caused by one typical infectious free EBV particle in a populaion consisting of naïve B cells [110, 111]. In general, a basic reproduction number

greater than one leads to persistent infection. Using the next generation matrix approach [110,111], we derived the basic reproduction number R_0 of our model to be

$$R_0 = \frac{n(1-\beta)\mu_e\lambda_n\omega_g\omega_d\omega_m}{\delta_e\delta_n(w_g+\delta_g-r_g)(w_d+\delta_d-r_d)(w_m+\delta_m-r_m)}, \text{ where } R_0 > 0. \tag{2.10}$$

Uisng parameter values in Table 2.1, we estimated R_0 to be 4.75. The basic reproduction number being greater than one implies that our model predicts the long-term persistence of EBV infection. This agrees with the profile of EBV infection shown in Figure 2.2. Our result supports findings on viral persistence in earlier model studies [88–90] and further validates that the Germinal Center Model can explain EBV persistence.

The expression of R_0 in equation 2.10 also shows the impact on the basic reproduction number of events during the expression of growth program, default program and latent program of EBV. The effect of NK cells modeled by the parameter β has a direct impact on the value of R_0.

2.4.3 Immunologic and virologic changes during primary EBV infection

A clinical study of Balfour *et al.* [106] analysed kinetic analysis of immunologic and virologic changes during primary Epstein-Barr virus (EBV) infection. The analysis was based on whole blood samples of subjects at time points from 50 days prior to and 100 days after onset of symptom. The symptom was re-

ported to have occurred in subjects two weeks prior to peak time of CD8 T cells (Figure 4A of [106]). We used LHS samples to simulate the profiles of free EBV load and aggregate CTL response to infected proliferating, germinal and lytic B cells. CTL pattern shows that the infection peaks at about six weeks post-infection after which the cells resolve to a low level of persistence, see Figure 2.3a. The peak time of CTL cells coincides with the peak time of oral cells EBV, see Figure 2.3a and Figure 2.3b. As shown in Figure 2.3b, our simulation results replicated the observed clinical observations of [106] on oral EBV cells during primary EBV infection.

2.4.4 Multiple peaks and decay of infected memory B cells and CTL cells

Clinical observation showed that both infected memory B cells and CTL cells specific to lytic B cells decay in parallel in the first five to six weeks after infectious mononucleosis patients report to clinic [86, 106]. Our simulation result replicates the observed parallel decay (see Figure 2.4), and this further suggests that both CTL and infected B_m peak about same time. This results has clinical significance as most primary EBV-infected patients report to clinics fater viral peak period [86]. In addition, we showed that variations in proliferation rate r_m of infected memory B cells can also reduce or elongate time to set-point for infected memory B cells, in addition to the CTL-centric alternative explanation provided in [86].

Our simulations also showed multiple peaks in the viral profile when $r_m = 0.0027$. Multiple peaks have been observed in clinical data [107].

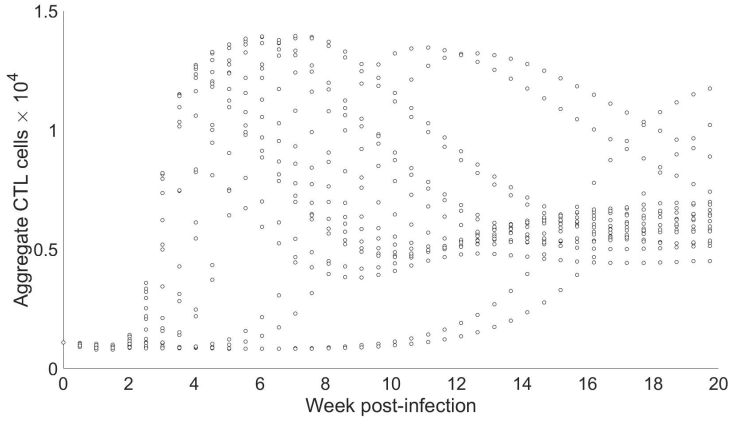

(a) Profiles of aggregate CTL response to infected proliferating, germinal and lytic B cells.

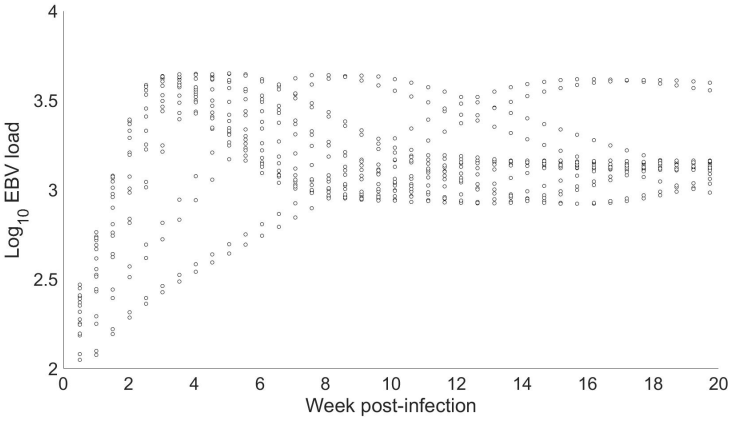

(b) Profile of simulated oral cells or free EBV load.

Fig 2.3. Simulated kinetics of CTL response and blood viral loads using thousand LHS samples of model parameters in equations 3.1–3.9.

2.4.5 Kinetics of infected memory B cells

Our sensitivity analysis showed that the rate ω_d at which the infected default B cells convert to infected memory B cells appeared to have a strong positive correlation with the peak value of infected memory B cells, Figure 2.5a. The activation rate r_2 of CTLs specific to the germinal center have a strong negative correlation with peak memory B cells, Figure 2.5a. The rate r_d at

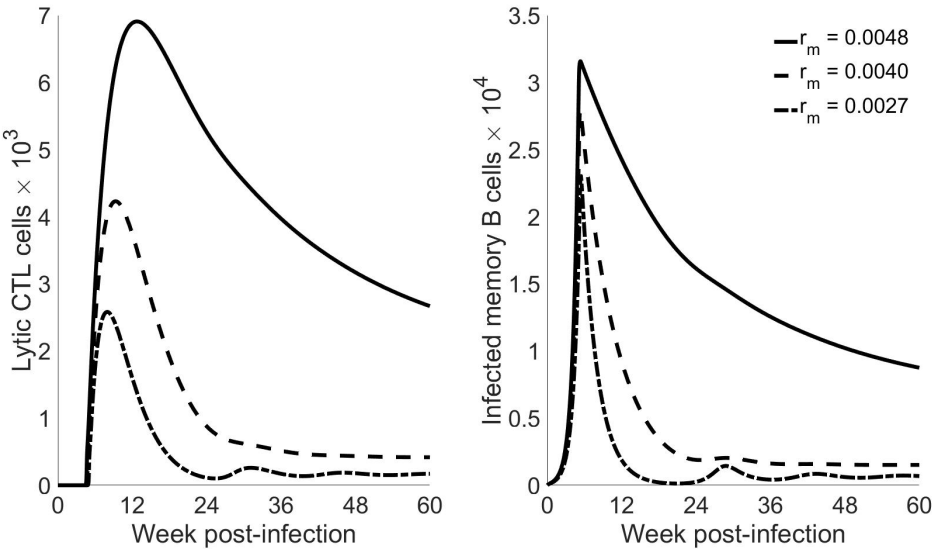

Fig 2.4. Model replicates parallel decay of infected memory B cells and CTL cells specific to lytic B cells.

which default B proliferates and infection rate μ_e of EBV have a strong negative linear relationship with memory B_m time to peak and the rate ω_d had a strongly positive correlation with B_m time to peak, Figure 2.5b. We observed a strong negative linear relationship between set-point of infected memory B cells and the activation rate r_2 of CTLs specific to the germinal center or the rate ω_m at which infected memory B cells reactivate into lytic B cells, Figure 2.5c. These correlations were all significant at (significance level $\alpha = 0.001$). We observed a weak linear relationship between time to set point of infected memory B cells and the death rate d_2 of CTLs specific to the germinal center, Figure 2.5d.

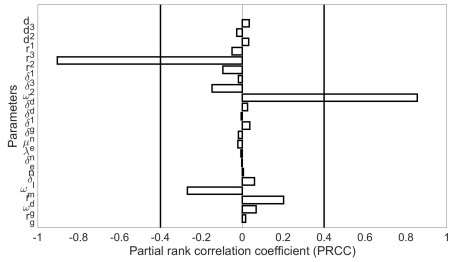

(a) Peak B_m

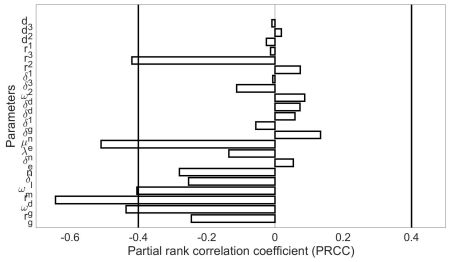

(b) B_m time to peak

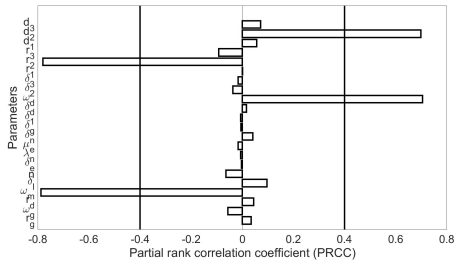

(c) B_m set-point

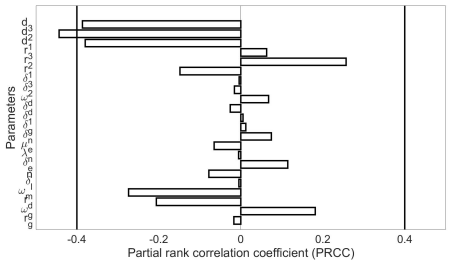

(d) B_m time to set-point

Fig 2.5. Model parameters and their correlation with peak, time to peak, setpoint and time to set point for the B_m compartment. The horizontal axis shows the partial correlations.

2.4.6 Short-term treatment fails to clear infected memory B cells

Our model showed that short-term treatment failed to impact peak, time to peak, set-point or time to set-point of infected memory B cells, Figure 2.6. Valganciclovir and acyclovir are some of the antiviral drugs that have *in vitro* activity against EBV. These drugs are unable to significantly reduce EBV load in the blood during short-term treatment [105]. We simulated short-term treatment with our model by varying the viral burst size n in equation 3.1 to reflect different treatment efficiencies. We chose six months as treatment window starting close to the peak time. For example, a $x\%$ efficient treatment for a period of eight weeks was simulated by fixing the viral burst size at $1-x\%$

of its value prior to treatment start time until the end of treatment schedule. We observed similar results when treatment window was between three and six months.

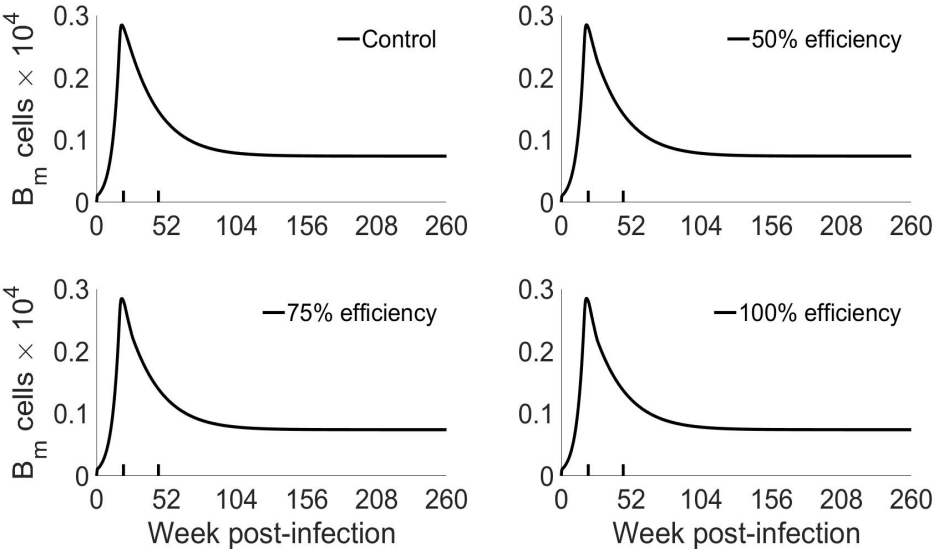

Fig 2.6. Short-term treatment fails to impact peak, time to peak, set-point or time to set-point of infected memory B cells. Short spikes on the x-axis indicate treatment start or end time.

2.4.7 Long-term treatment impacts set-point of memory B cells

Hoshino *et al.* [95] speculated that a long-term EBV-specific valganciclovir treatment could clear the memory B cells compartment of EBV if the host is not reinfected by an exogenous virus [95, 105]. We investigated the effects of long-term antiviral treatment using our model by setting the proliferation rate r_g to 0.378 per week, the CTL killing rate δ_1 to 229.82 per week and varying the burst size n to simulate $50\%, 75\%$ and 100% efficiency of the antiviral treatment starting at five weeks prior to peak viral load for a period of four

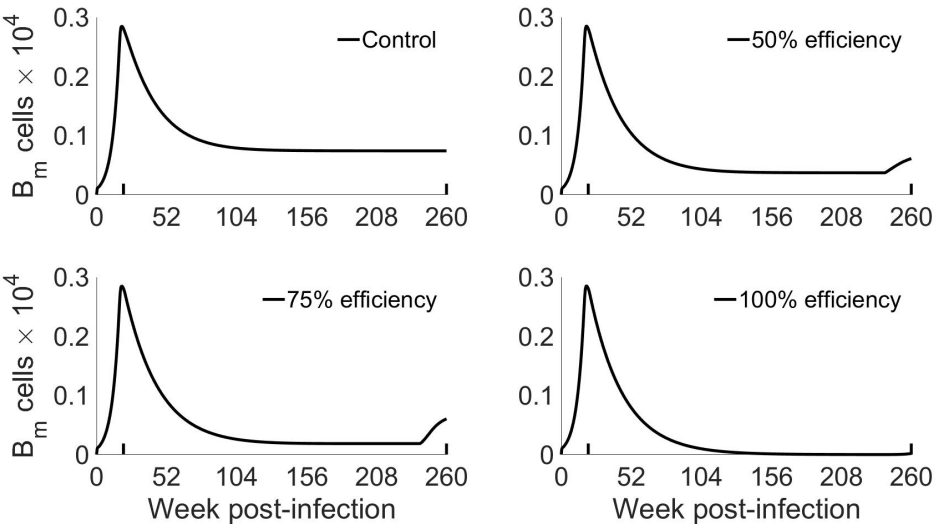

Fig 2.7. Long-term treatment impacts set-point of memory B cells kinetics when treatment. Short spikes on the x-axis indicate treatment start or end time.

and half years. This resulted in a significantly lower set-point in all EBV-infected compartments, in particular the B_m compartment, after the first peak (Figure 2.7) and EBV compartment was cleared during the treatment period as speculated by Hoshino *et al.* [95]. We observed similar patterns when treatment length was varied from one to four years. The patterns in Figure 2.7 suggests a during-treatment clearance in the infected cell compartments. The set-point was similarly impacted when treatment efficiency was between 50% and 100% but with a possible relapse prior to end of treatment.

2.4.8 The impact of innoculum size

We tested the impact of innoculum size by varying the initial size of EBV infectious particles. Innoculum appeared to effect only the peak value of each compartment, with the exception of naïve B cells compartment, and time to peak for all compartments, see Figure 2.8 and Figure 2.9. An increase in

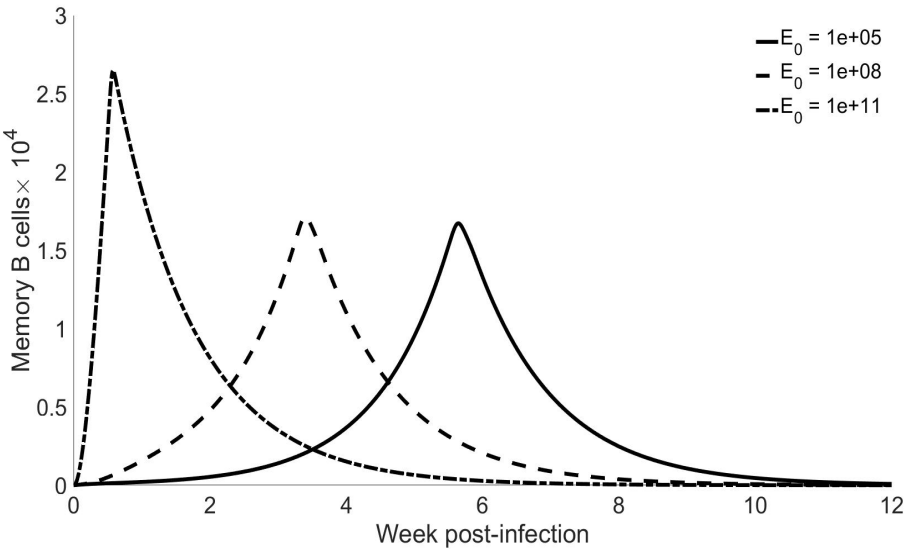

Fig 2.8. Increasing innoculum size impacts peak value and time to peak for EBV-infected memory B cells.

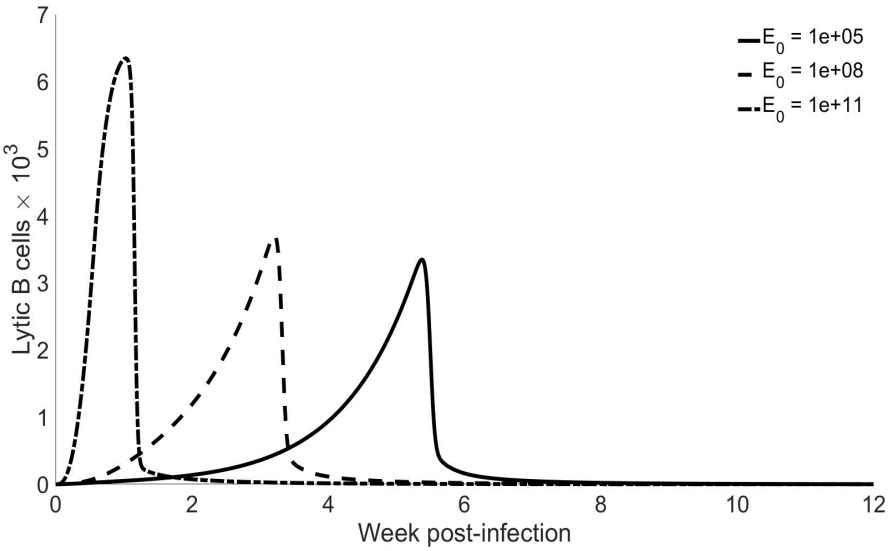

Fig 2.9. Increasing innoculum size impacts peak value and time to peak for lytic B cells.

the innoculum size increased the peak values of latently infected memory B cells and lytically infected B cells, and reduced the corresponding times to peak for each compartment. Their set-points and times to set-point appeared

not to be effected by innoculum size. We observed similar results for other compartments.

Chapter 3

Impacts of Immunosuppressive Therapy and Antiviral Treatment on EBV Kinetics in Transplantation

3.1 Introduction

There is a need to translate how viral infections alter alloreactivity in transplant recipients to improve clinical outcomes of transplantation while adjusting for integrity of protective immunity to pathogenic molecular patterns. Lifelong immunosuppression of transplant recipients can give rise to opportunistic infections and reactivation of latent viral infections such as Epstein-Barr virus more frequently within the first year of transplantation [114, 152, 153]. The Epstein-Barr virus (EBV) genome is prevalent in more than 90% of B cell-

associated complications of solid organ transplantation [148]. EBV's ability to transform B lymphocytes is the leading cause of these disorders [113–115,148].

Immunosuppressive drugs alter immune responses, particularly EBV-directed cytotoxic T lymphocytes response, and survival of EBV-infected cells during transplantation [148]. Immunosuppression is typically expected to result in peak viral loads, possibly setting the stage for malignancy and allograft rejection. Advancement in the development of immunosuppressive drugs has resulted in long-time survival of transplant recipients. Acute rejection rates and 1-year survival rates were at about 60% between 1970s and early 1980s and by mid-1980s rejection rates decreased to $40 - 50\%$ and 1-year survival rates increased to $75 - 85\%$ [131]. A 3-signal model has been proposed for T-cell activation and proliferation and newer immunosuppressive medications target relevant co-stimulatory pathways of this model [147] while minimising proximal toxicities. Intense immunosuppression is usually required immediately after the placement of allograft to minimise the risk of rejection and this class of medications are referred to as "induction agents" [131, 151]. These agents are mostly used in combination with maintenance immunosuppressive drugs at lower doses when less immunosuppression is required post-transplant [131, 147, 151].

Strategy for optimal immunosuppression therapy remains unclear and current understanding of relevance of immunosuppression to kinetics of EBV-infected cells in transplant recipients is limited. Optimal outcome of transplantation in patients with active EBV infection can depend on insights from the contribution of each induction agent as well as their timing and dose. We used mathematical models of primary EBV infections developed in [116, 137]

and mathematical models of immunosuppressive drugs [124, 132] to investigate impacts of transplant treatments on the kinetics of EBV infection in transplant context with the objective of identifying parameters that modulate peak values, peak times, set points and times to set points for all model compartments. We focused on maintenance immunosuppressive drugs (tacrolimus, mycophenolate and prednisone) and induction agents (basiliximab and rabbit antithymocyte globulin) with valganciclovir.

3.2 Methods

Epstein-Barr virus (EBV) primary infection has been represented by the Germinal Center Model (GCM) proposed by Thorley-Lawson et al. [113–115]. We investigated the impacts of immunosuppression on EBV kinetics in transplant settings by coupling a mathematical model of GCM [116] with mathematical models of common immunosuppressive drugs used by solid organ recipients.

3.2.1 Mathematical Model

The mathematical model of GCM is characterised by nine interacting agents: free EBV virions E, naïve B cells B_n, infected B cells B_g expresing growth program, infected B cells B_d expressing default program, infected memory B cells B_m, lytically infected B cells B_l, cytotoxic T lymphocytes (CTLs) T_g specific to infected B cells expressing growth program, CTLs T_d specific to infected B cells expressing default program and CTLs T_l specific to lytically infected B cells. The mathematical model has been described in detail in the previous chapter and we give an overview of the dynamics of these agents

below.

Lytically infected B cells B_l release infectious EBV E at a rate δ_l with burst size n and the free virus has turnover rate δ_e as in equation 3.1. In equation 3.2, naïve B cells B_n are produced at a constant rate λ_n with turnover rate δ_n, and are infected by EBV particles E at a rate μ_e to become infected B cells B_g expressing growth program. Infected B cells B_g die at a rate δ_g, are rescued into the germinal center at a rate ω_g, proliferate at a rate r_g with NK cells effect on their production rate modeled by $1-\beta$ as in equation 3.3 and T_g lymphocytes eliminate these cells at a rate δ_1.

The B_g cells are transformed into infected B cells B_d expressing default program at a rate ω_g, which has net proliferation rate $(r_d - \delta_d - \omega_d)$, and are elimnated by T_d lymphocytes at a rate δ_2, equation 3.4. A fraction of infected B cells expressing default program transforms into infected memory B cells B_m at a rate ω_d and the net proliferation rate of B_m is modeled by $(r_m - \omega_m - \delta_m)$. Lytically infected B cells B_l are produced from infected memory cells at a rate ω_m, undergo apoptosis at a rate δ_l and are eliminated by T_l lymphocytes at a rate δ_3. The respective production rates of T_g, T_d and T_l are r_1, r_2 and r_3 with turnover rates given by d_1, d_2 and d_3 respectively.

$$\frac{dE}{dt} = (1 - e_V(t))n\delta_l B_l - \delta_e E, \tag{3.1}$$

$$\frac{dB_n}{dt} = \lambda_n - \mu_e E B_n - \delta_n B_n, \tag{3.2}$$

$$\frac{dB_g}{dt} = (1 - \beta\,(1 - \varepsilon_{\mathrm{a}}(t)))\mu_e E B_n + (r_g - \omega_g - \delta_g)\,B_g - \delta_1 T_g B_g, \tag{3.3}$$

$$\frac{dB_d}{dt} = \omega_g B_g + (r_d - \delta_d - \omega_d)B_d - \delta_2 T_d B_d, \tag{3.4}$$

$$\frac{dB_m}{dt} = \omega_d B_d + (r_m - \omega_m - \delta_m) B_m, \tag{3.5}$$

$$\frac{dB_l}{dt} = \omega_m B_m - \delta_l B_l - \delta_3 T_l B_l, \tag{3.6}$$

$$\frac{dT_g}{dt} = (\varepsilon_{\mathrm{b}}(t) - 1)\,(1 - \varepsilon_{\mathrm{m}}(t))\, r_1 T_g B_g - d_1 T_g - (1 - \varepsilon_{\mathrm{a}}(t))\, T_g, \tag{3.7}$$

$$\frac{dT_d}{dt} = (\varepsilon_{\mathrm{b}}(t) - 1)\,(1 - \varepsilon_{\mathrm{m}}(t))\, r_2 T_d B_d - d_2 T_d - (1 - \varepsilon_{\mathrm{a}}(t))\, T_g, \tag{3.8}$$

$$\frac{dT_l}{dt} = (\varepsilon_{\mathrm{b}}(t) - 1)\,(1 - \varepsilon_{\mathrm{m}}(t))\, r_3 T_l B_l - d_3 T_l - (1 - \varepsilon_{\mathrm{a}}(t))\, T_l. \tag{3.9}$$

The dynamic treatment parameters $\varepsilon_{\mathrm{m}}(t), \varepsilon_{\mathrm{b}}(t), \varepsilon_{\mathrm{a}}(t)$ and $\varepsilon_{\mathrm{V}}(t)$ are discussed in the next section.

3.2.2 Therapeutics

Immunosuppressive drugs are generally classified into two types - induction agents and maintenance medications - based on timing. Induction agents refer to those drugs used in the first few days or weeks post-transplant and they function either as lymphocyte depleting agents or lymphocyte inhibitory agents. Basiliximab and antithymocyte globulin are two common examples of induction agents. Maintenance drugs are used at lower doses for the rest of a recipient's lifetime or the allograft's lifetime to prevent organ rejection [117, 118, 131, 147].

Maintenance Immunosuppression

Standard maintenance immunosuppressive regimen is a three-drug combination that simultaneously targets various levels of immune response cascade [117, 130, 131, 147] to disrupt T-cells activation process. Calcineurin inhibitors such as tacrolimus and cyclosporine, and sirolimus, a mammalian target of rapamycin (mTOR) inhibitor, are commonly used maintenance im-

munosuppressants and they all have antiproliferative effects on immune response [117, 131, 147]. The triple regimen of tacrolimus, mycophenolate, and prednisone is the most common maintenance regimen [147]. Tacrolimus is an inhibitor of calcineurin, a molecule that is required for downstream activation of immune response [117, 131, 147]. Mycophenolate is an antiproliferative that is available in two formulations - mycophenolate mofetil (MMF, CellCept) and mycophenolic acid (MPA, MyFortie) - and both inhibit purine base synthesis required for T- and B-cell proliferation [131, 147]. Prednisone is a corticosteroid that is metabolised in the liver to prednisolone and exhibits anti-inflammatory and immunosuppressive activity by inhibiting T-cell-derived and antigen-presenting cell-derived cytokine expression and leads to antiproliferative effect [131, 147].

We used

$$\varepsilon_{\mathrm{m}}(t) = \begin{cases} \mathrm{m}_{\max} & : 0 \leq t \leq t_0 \\ \mathrm{m}_{\max} + \frac{\mathrm{m}_{\min} - \mathrm{m}_{\max}}{t_1 - t_0}(t - t_0) & : t_0 \leq t \leq t_1 \\ \mathrm{m}_{\min} & : t_1 \leq t, \end{cases} \tag{3.10}$$

in equations 3.7-3.9 to model effects of mainetanance drugs. The $\mathrm{m}_{\max}$ represents the initial efficacy of a maintenance regimen which we presume lasts for time t_0 and wanes at a rate given by

$$\frac{\mathrm{m}_{\min} - \mathrm{m}_{\max}}{t_1 - t_0} \tag{3.11}$$

in period $t_1 - t_0$ before dropping to baseline $\mathrm{m}_{\min}$ after time t_1.

Basiliximab

Basiliximab is a non-depleting, chimeric monoclonal antibody that antagonises IL-2 receptor CD25. Signaling through CD25 initiates a kinase-dependent cascade that leads to T-cell proliferation and differentiation, as a consequence basiliximab has inhibitory effects with mean duration of 4-6 weeks and does not cause T-cell depletion [117, 131, 135, 147].

We used

$$\varepsilon_{\mathrm{b}}(t) = \begin{cases} \mathrm{b}_{\min} & : 0 \leq t \leq t_0 \\ \mathrm{b}_{\min} + \frac{\mathrm{b}_{\max} - \mathrm{b}_{\min}}{t_1 - t_0}(t - t_0) & : t_0 \leq t \leq t_1 \\ \mathrm{b}_{\max} & : t_1 \leq t, \end{cases} \tag{3.12}$$

in equations 3.7-3.9 to model effects of basiliximab. The $\mathrm{b}_{\min}$ represents the initial efficacy of basiliximab which we presume lasts for time t_0 and grows at a rate given by

$$\frac{\mathrm{b}_{\max} - \mathrm{b}_{\min}}{t_1 - t_0} \tag{3.13}$$

before reaching a homeostatic level of $\mathrm{b}_{\max}$ after time t_1.

Antithymocyte Globulin

Antithymocyte globulins (ATGs) are immunoglobulin G (igG) from horses or rabbits immunised with human thymocytes. ATG targets multiple markers such as CD4 and CD8, T and B cells as well as MHC molecules and natural killer (NK) cells and depletes harmful T cells [129, 131, 147]. T cells, NK cells, monocytes, macrophages, dendritic cells, naïve B cells and a susbset of activated B cells are also targeted by ATG. ATG has been found strongly to induce

apoptosis against naïve B cells, activated B cells and bone marrow resident plasma cells [129]. CD80, a marker expressed on EBV-activated naïve B cells that express the growth program, has been implicated in ATG activity [129].

We used

$$\varepsilon_{\mathrm{a}}(t) = \begin{cases} \mathrm{a_{min}} & : 0 \leq t \leq t_0 \\ \mathrm{a_{min}} + \frac{\mathrm{a_{max}} - \mathrm{a_{min}}}{t_1 - t_0}(t - t_0) & : t_0 \leq t \leq t_1 \\ \mathrm{a_{max}} & : t_1 \leq t, \end{cases} \tag{3.14}$$

in equations 3.3 and 3.7-3.9 to model effects of ATG.

In equation 3.14, 1-$\mathrm{a_{min}}$ represents the initial effect of ATG which we presume lasts for time t_0 and wanes at a rate given by

$$\frac{\mathrm{a_{max}} - \mathrm{a_{min}}}{t_0} \tag{3.15}$$

before reaching a homeostatic level of $1 - \mathrm{a_{max}}$ after time t_1.

We simplified our model by assuming that ATG targets only the CTL compartments and NK cells.

Valganciclovir

Ganciclovir is a potent inhibitor of viruses of the herpes family, including EBV [126], and valganciclovir is a valine ester prodrug of ganciclovir developed to overcome the limitations of oral and IV ganciclovir [127]. We modeled valganciclovir concentrations after uniform multiple oral dosing as [124, 132]

$$C_V(t) = \begin{cases} \frac{D_V k_a}{V_V(k_a - k_{el})} \left[\frac{1-e^{-n_V k_{el} \tau_V}}{1-e^{-k_{el}\tau_V}} e^{-k_{el}t} - \frac{1-e^{-n_V k_a \tau_V}}{1-e^{-k_a \tau_V}} e^{-k_a t} \right] & : t_{\text{start}} \leq t \leq t_{\text{end}} \\ 0 & : \text{otherwise,} \end{cases} \tag{3.16}$$

where D_V denotes dose, τ_V is the dosing interval, n_V is the number of doses, t is the time since the last dose, V_V denotes volume of distribution, k_a denotes absorption rate constant, k_{el} denotes elimination rate constant, and t_{start} and t_{end} are treatment start time and duration of treatment. We model the efficiency of valganciclovir at time t by

$$e_V(t) = \varepsilon_V \frac{C_V}{C_V + \text{IC}_V}, \tag{3.17}$$

where ε_V is the maximum valganciclovir efficiency and IC_V is the valganciclovir concentration that will produce 50% efficiency.

Ganciclovir phosphorylates to competitively inhibit viral DNA by acting as an analog to deoxyguanosine triphosphate (dGTP) and consequently inhibits the replication of herpes simplex viruses such as EBV [126]. We model this effect by using equation 3.17 in equation 3.1.

3.2.3 Simulation

We used the parameters in Table 2.1 together with the pharmacokinetic parameters in Table 3.1 to simulate equations 3.1–3.9 in this work. We used Matlab [162] for the simulation. We coupled the maintenance immunosuppression equation 3.10 with the basiliximab equation 3.12 or antihymocyte globulin

equation 3.14 with or without antiviral equation 3.17 to simulate equations 3.1-3.9. We assumed that antiviral treatment was adminsitered at transplanation for 3 months, 6 months or 9 months duration. We investigated innoculum size effect when maintenance immunosuppression is combined with basiliximab or antithymocyte globulin. Similar to the sensitivty approach that we used in chapter 2, we used Latin Hypercube Sampling (LHS) [116] to sample innoculum size in the interval $[5 \times 10^4, 2 \times 10^5]$ with treatment parameters set at the baseline and we used partial correlation coefficient method to measure the correlations reported in Table 3.2 and Table 3.3. We used significance level $\alpha = 0.05$ for Pearson correlation coefficient. We plotted the immunosuppressive functions that we used in the simulation in Figure 3.1.

3.3 Results

The typical primary infection profile is that the free EBV and the infected memory B cells compartments peak at about five weeks post primary infection with a mild second peak at about 32 weeks post-infection [116,136]. This profile was observed in all model compartments in [116]. In this work we investigate how innoculum size, immunosuppressive drugs, and antiviral treatment affect peak time, peak values, time to setpoint and setpoint values in all model compartments.

3.3.1 ATG increases risk of EBV-associated complications

High viral load has been reported to correlate with risk of EBV-associated complications post-transplant [148,149]. We observed that peak infected mem-

ory B cells and peak free EBV increased by about 7% and about 11% respectively when antihymocyte globulin was used in combination with maintenance immunosuppression compared to the 1.9×10^5 peak memory B cells and 1.6×10^9 peak EBV with basiliximab, Table 3.4 and Figure 3.2a-Figure 3.2d. ATG increased time to peak infected memory B cells and time to peak EBV by about 60% (compared to 2.5 months with basiliximab), increased setpoint of infected memory B cells by about 40% (compared to 270 with basiliximab), and increased time to setpoint by about 25% (compared to 12 months with basiliximab), Table 3.4 and Figure 3.2a-Figure 3.2d. The profiles of CTLs appeared to follow clinical pattern of immune reconstitution after induction and maintenance immunosuppression treatments [159–161]. Immune reconstitution was delayed for about a month followed by a snap peak that parallels peak times in both EBV and infected memory compartments, Figure 3.2e-Figure 3.2h. The observed patterns of CTL reconstition under ATG appeared similar to that of basiliximab. We observed similar CTL profiles for CTLs specific to the infected proliferating B cells.

3.3.2 Valganciclovir treatment reduces peak viral load and peak memory B cells

We only report the results of antiviral treatment at transplantation with 6 months treatment duration and 50% antiviral drug efficiency because we observed similar results with 3 months and 9 months treatment durations, and 60%, 75% and 90% antiviral drug efficiency. Maintenance immunosuppression and induction agent with or without antiviral treatment immediately after transplantation had similar time to setpoint and setpoint in all model

compartments regardless of treatment duration, Table 3.4.

We observed 10% increase in peak infected memory B cells with ATG compared to the 1.01×10^5 with basiliximab and the time to peak infected memory B cells and time to peak EBV was about 3 months for both ATG and basiliximab. Antiviral treatment reduced peak memory B cells by about 47% and peak EBV by about 83% respectively compared to the 1.9×10^5 peak memory B cells and 1.6×10^9 peak EBV when basiliximab was used without antiviral, Table 3.4 and Figure 3.3c vs Figure 3.2c. Antiviral treatment reduced peak memory B cells by about 30% and peak EBV by about 74% respectively compared to the 1.5×10^6 peak memory B cells and 1.9×10^{10} peak EBV and reduced time to peak memory B cells by about 25% when ATG was used without antiviral, Table 3.4 and Figure 3.3d vs Figure 3.2d.

3.3.3 Innoculum size increases peak and setpoint, and lowers time to peak and setpoint

We observed perfect positive correlation between both peak and setpoint for each model compartment and innoculum size, Table 3.2, when we varied innoculum size under maintenance immunosuppression and basiliximab treatment, and we observed a perfect negative correlation between both time to peak and time to setpoint for each model compartment and innoculum size, Table 3.2. The correlation patterns in infected B cells compartments and EBV compartment with antithymocyte globulin were similar to those observed under basiliximab treatment, Table 3.3. We observed negative correlations between innoculum size and all the kinetic parameters for the cytotoxic compartments, Table 3.3.

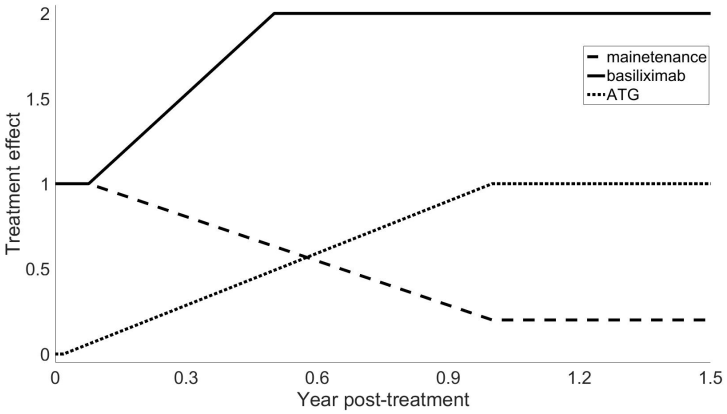

Fig 3.1. Plots of maintenance immunosuppression, basiliximab and antithymocyte treatment functions

Supporting Information

Table 3.1. Treatment parameters used in simulations of equations 3.1–3.9.

Treatment	Variable	Description	Value/Range	Reference
	m_{max}	Maximum efficiency	100%	
	t_0	Start of efficiency decay	28 days	
Maintenance	t_1	Time to baseline efficiency	1 year	[159–161]
	m_{min}	Baseline efficiency	20%	
	b_{max}	Maximum effect	200%	
	t_0	Start of effect expansion	28 days	
Basiliximab	t_1	End of effect expansion	6 months	[159–161]
	b_{min}	Initial effect	100%	
	a_{min}	Initial level	0%	
	t_0	Time to CTL depletion	7 days	
ATG	t_1	Time to homestatic level	1 year	[159–161]

	a_{max}	homeostatic level	100%	
Valganciclovir	D_V	Dose	900mg	
	V_V	Volume of distribution	42.6L	
	ε_V	Maximum valganciclovir efficiency	$[5\%, 100\%]$	
	k_a	Absorption rate	3 per hour	
	k_{el}	Elimination rate	14.5 per hour	
	n_V	Number of doses	1 dose	[126, 139]
	τ_V	Dosing interval	24h	
	t_{start}	Treatment start time	1 day	
	t_{end}	Treatment duration	$[85, 954]$ days	
	IC_V	50% inhibitory concentration	1.0μM	

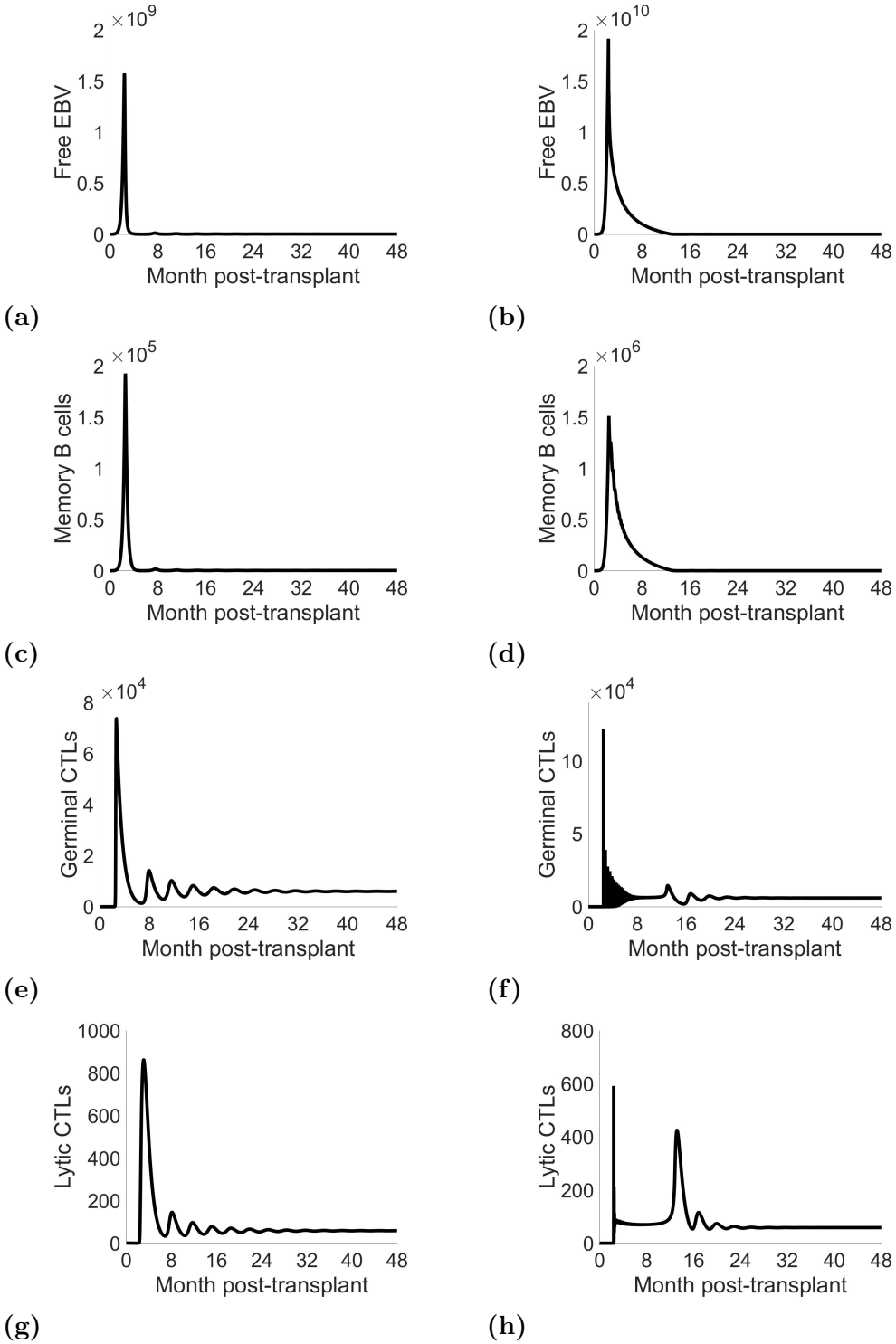

Fig 3.2. Impacts of maintenance immunosuppression and induction agents on kinetics of EBV infection of donor organ. Figures on the left panel reflect impacts of basiliximab treatment and those on the right reflect impacts of ATG treatment.

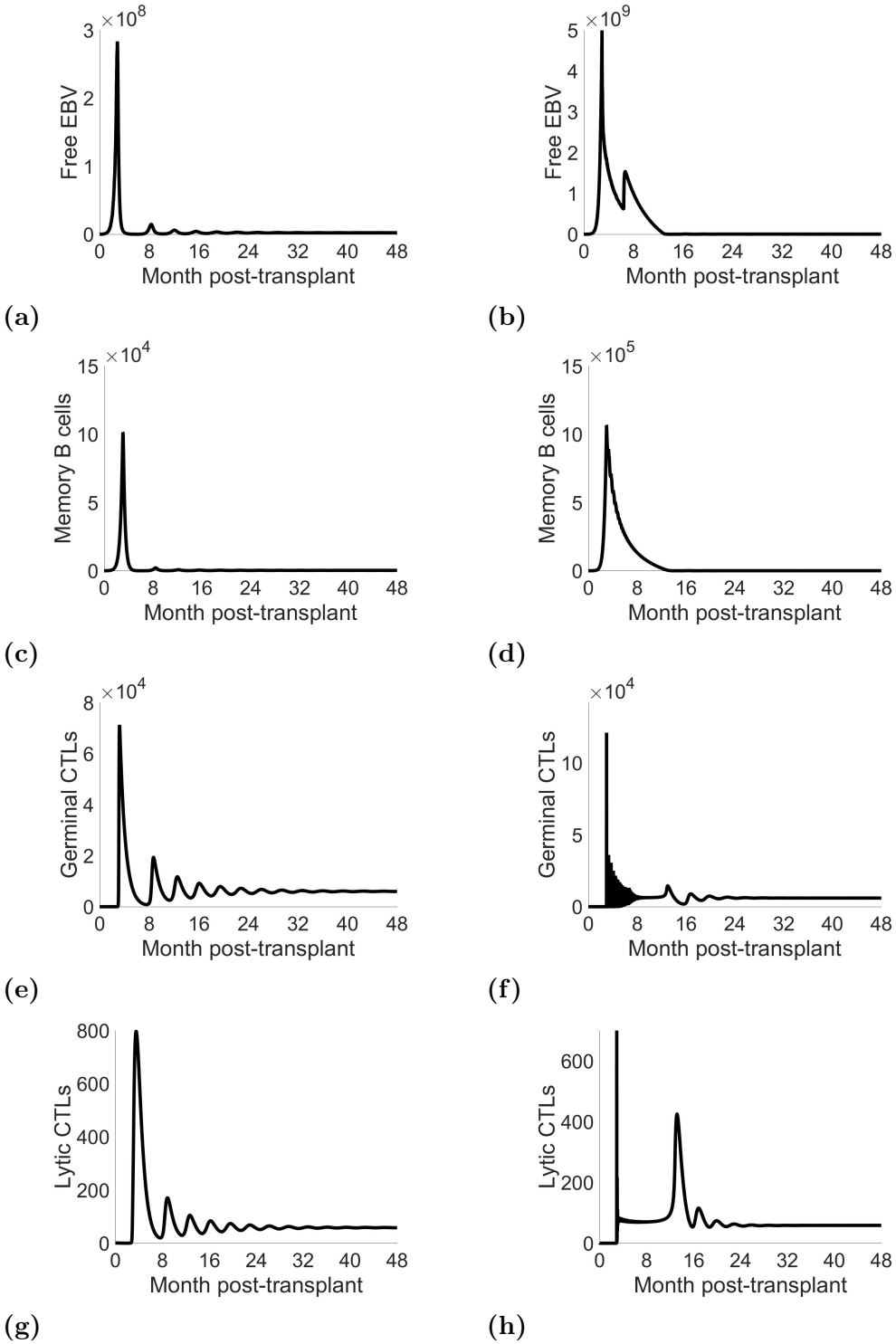

Fig 3.3. Impacts of maintenance immunosuppression, induction agents and 6 months, 50% efficient valganciclovir treatment on kinetics of EBV infection of donor organ immediately after transplantation. Figures on the left panel reflect impacts of basiliximab treatment and those on the right reflect impacts of ATG treatment.

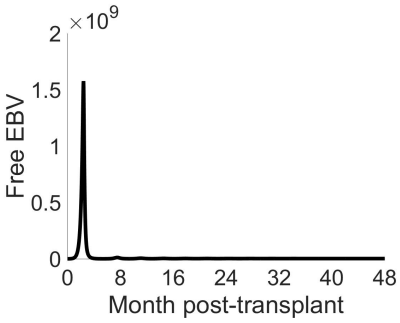
×10^9
2
1.5
1
0.5
0
Free EBV
0
8
16
24
32
40
48
Month post-transplant

(a)

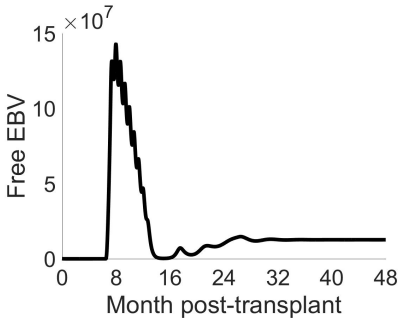
×10^7
15
10
5
0
Free EBV
0
8
16
24
32
40
48
Month post-transplant

(b)

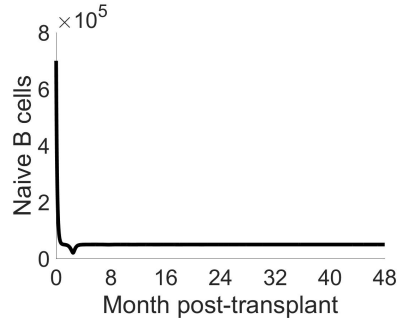
×10^5
8
6
4
2
0
Naive B cells
0
8
16
24
32
40
48
Month post-transplant

(c)

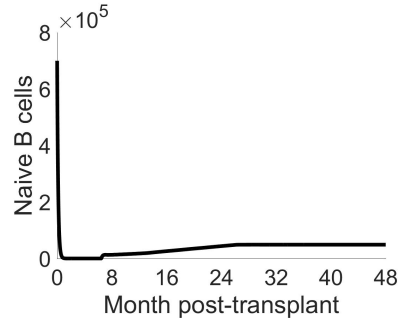
×10^5
8
6
4
2
0
Naive B cells
0
8
16
24
32
40
48
Month post-transplant

(d)

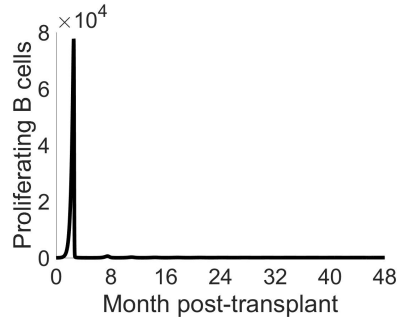
×10^4
8
6
4
2
0
Proliferating B cells
0
8
16
24
32
40
48
Month post-transplant

(e)

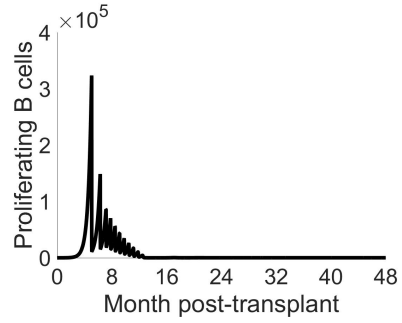
×10^5
4
3
2
1
0
Proliferating B cells
0
8
16
24
32
40
48
Month post-transplant

(f)

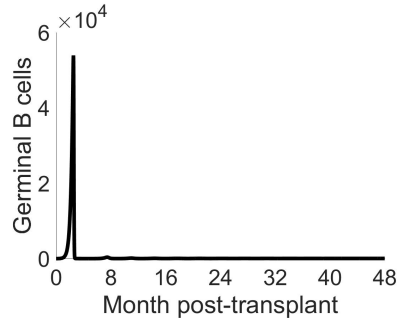
×10^4
6
4
2
0
Germinal B cells
0
8
16
24
32
40
48
Month post-transplant

(g)

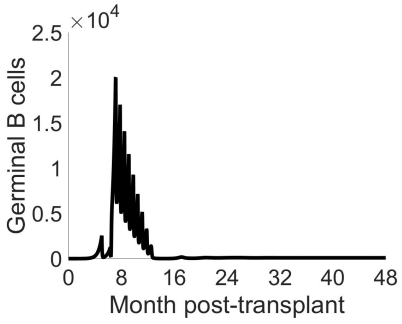
×10^4
2.5
2
1.5
1
0.5
0
Germinal B cells
0
8
16
24
32
40
48
Month post-transplant

(h)

Table 3.2. Correlation between peak, time to peak, setpoint or time to setpoint and innoculum EBV with maintenance immunosuppression and basiliximab treatment.

Compartment	Peak	Peak time	Setpoint	Time to setpoint
EBV	99.8%	-99.5%	88.6%	-99.5%
B_g	87.8%	-79.4%	72.5%	-89.7%
B_d	68.4%	-58.9%	89.1%	-86.5%
B_m	79.7%	-70.2%	63.8%	-69.3%
B_l	83.5%	-76.3%	79.8%	-99.1%
T_g	100.0%	-92.5%	100.0%	-59.5%
T_d	100.0%	-99.5%	100.0%	-79.5%
T_l	99.8%	-95.4%	99.8%	-99.5%

Table 3.3. Correlation between peak, time to peak, setpoint or time to setpoint and innoculum EBV with maintenance immunosuppression and ATG treatment.

Compartment	Peak	Peak time	Setpoint	Time to setpoint
EBV	99.3%	-79.0%	99.3%	-79.0%
B_g	17.0%	-63.9%	45.5%	-63.9%
B_d	99.7%	-99.2%	99.6%	-99.2%
B_m	99.4%	-99.3%	99.4%	-99.3%
B_l	99.0%	-82.1%	99.0%	-82.1%
T_g	-69.8%	-99.2%	-18.2%	-99.2%
T_d	-57.2%	-81.2%	-39.2%	-76.8%
T_l	-68.5%	-88.2%	-25.0%	-68.9%

Table 3.4. Values of peak, time to peak, setpoint and time to setpoint under immunosuppressive and antiviral treatments.

Compartment	Treatment	Peak	Time to peak	Setpoint	Time to setpoint
Memory B cells	ATG	1.5×10^6	4 mo.	378	15 mos.
	Basiliximab	1.9×10^5	3 mos.	270	12 mos.
	ATG + Antiviral	1.07×10^6	3 mos.	377	15 mos.
	Basiliximab + Antiviral	1.01×10^5	3 mos.	270	12 mos.
EBV	ATG	1.9×10^{10}	4 mos.	3.1×10^6	15 mos.
	Basiliximab	1.6×10^9	3 mos.	2.2×10^6	12 mos.
	ATG + Antiviral	5.0×10^9	3 mos.	3.0×10^6	15 mos.
	Basiliximab + Antiviral	2.8×10^8	3 mos.	2.1×10^6	12 mos.

Chapter 4

Conclusions, Limitations and Extensions

4.1 Discussion

Primary EBV infection is known to peak in about five to six weeks and this is close to model simulated profile. We have shown that the infection rate of EBV and the proliferation rates of infected germinal B cells negatively correlate with infected memory B cells time to peak. As the memory compartment is being used as a surrogate for EBV load, this result suggests that the infection rate of EBV and the proliferation rate of B_d should be targeted to lower the peak time of infected memory B cells. Similarly, our results suggest that interfering with the pathway from the germinal compartment to the memory compartment is a key factor for reducing the peak level of infected memory B cells. We have also shown that early and intense specific CTL response significantly lowers the peak level of infected memory B cells.

We showed that innoculum size impacts peak value, with the exception of naïve B cells, and time to peak for all model compartments. It is known that EBV symptoms occur in subjects two weeks prior to peak time of CD8 T cells. It may be possible to use this information and the positive correlation between innoculum size and peak time to infer the innoculum size in a patient.

We showed that both short-term and long-term antiviral treatment failed to clear infected memory B cells from the system although long-term treatment clear free EBV during treatment period. We observed a transient clearance followed by a periodic rebound in the infected cell compartments caused by positive net proliferation rate of either the infected growth B cells or infected default B cells. This suggests that alternative treatments for EBV should be explored in addition to antiviral treatment if the goal is to eliminate persistent infection.

EBV viral proteins, the coordinated effects of viral and cellular miRNAs, and immunosuppressive drugs alter the proliferative response and survival of infected cells and EBV-specific cytotoxic T lymphocyte (CTL) responses critical for controling EBV infection [148, 149]. The objective of this work is to quantify the risk associated with rituximab treatment, antiviral treatment and specific immunosuppressive agents used for maintenance immunosuppression in transplantation. In addition to using viral load to monitor EBV-associated complications in transplant recipients [148,149], we propose the use of kinetics of EBV and EBV-infected (memory) B cells to monitor response to treatment. We have used a system of mathematical equations, based on a biological model of EBV infection, to investigate how the implications of this proposal relate to the risks of EBV-associated complications in transplant recipients.

We recommend the use of basiliximab as an indution agent with or without antiviral. Antithymocyte globulin (ATG) has historically been associated with increased risk of PTLD, a spectrum of EBV-associted complications in transplant recipients [148, 149]. In this study we found that ATG combined with maintenance immunosuppression increases peak and setpoint infected memory B cells, and peak and setpoint EBV load compared to the the use of basiliximab combined with maintenance immunosuppression. ATG also delays time to both EBV or infected memory B cells setpoint or peak. This result suggests that a low-dose of basiliximab that follows the profile in equation 3.12 should be an initial approach to management of EBV-associated complications in transplant recipients. It would result in a lower peak or setpoint EBV load and reduce time to setpoint or time to peak with a combined effect of lowering the risk of post-transplant EBV-associated diseases. We observed that basiliximab with or without valganciclovir has similar effects of kinetics of both memory B cells and free EBV.

4.2 Data challenges

The sites of infection and persistence of Epstein-Barr Virus, that is, B lymphocytes of Waldeyers ring (tonsils and adenoids) and the peripheral blood, allow measurements which can be used to derive parameter values and validate model of EBV infection. Our model is the first to consider all infection stages of EBV that have been demonstrated experimentally together with separate compartments for naïve B cells and EBV. As a consequence, we lacked data for the parameters of the new compartments that we added. In our model, we assumed the published biologically feasible parameter values used in the

agent-based computer simulation of EBV infection in Shapiro *et al.* study [88] and Huynh-Adler work [10, 89].

Our model of EBV infection is the first to be applied to investigate the kinetics of EBV in (solid organ) transplantation context. There is paucity of literature on the pharmacokinetics parameters of the drugs used to manage EBV in transplant recipients. Consequently, rather than use pharmacokinetic model and their pharmacokinetic parameters to represent these drugs, we designed mathematical equations that we "fitted" to the published profiles of these drugs or profiles of their targets cells in patients infected with or without EBV.

We believe that our model can be improved by using parameters estimated from Epstein-Barr viral loads and EBV-infected cell data obtained from infected humans diagnosed with infectious mononucleosis or who are solid organ transplant recipients.

4.3 Mathematical model challenges

The sites of EBV infection and persistence are localised, as such it is reasonable to think that EBV processes are spatially distributed through cell-to-cell viral transmission. If this thought holds true, the spatial homogeneity and well-mixed assumptions that underlie continuous models based on ordinary differential equations (ODE) could be improved by using a system of partial differential equations or any other spatial model that accounts for possible spatial heterogeneity of EBV infection process.

EBV is thought to target both B cells and epithelial cells within a host. The virus is thought to enter B cells and epithelial cells through different

glycoprotein complexes on its envelope [2–4]. The germinal center model that we based our work downplays the role of epithelial cells in EBV infection [1, 12, 87, 88]. Our model can be extended to account for possible roles of epithelial cells in EBV infection processed.

Most people get EBV infection at young age and are asymptomatic [1, 10, 18, 89]. Infectious mononucleosis(IM) is highly prevalent in adolescents and young adults suggesting possible age-dependence in EBV infection processes. Our model can be extended to account for the role of age in EBV kinetics in IM patients and solid organ transplant (SOT) patients. However, since CTL responses and NK responses are highly dependent on age, simulation of changes in these responses that have been described in children relative to adults using our model may allow up to examine age-related changes in the model in the future

Direct infection model (DIM) is an alternative to the germinal center model (GCM) of EBV infection. DIM, proposed by Kuppers and coworkers [5, 6], contends that EBV directly infects memory B cells, suggesting that there is no need for naïve B cells, proliferating B cells and germinal center B cells compartments, or there is a possibility of an additional direct interaction between Epstein-Barr virus and infected memory B cell. We note that although there is no sufficient experimental evidence to support DIM, our model can be extended to incorporate DIM.

We did not subdivide the reactivation of EBV into immediate early, early or late phase. The immediate early phase is when the transcription factors initiating viral replication are expressed, early phase is when the proteins involved in viral DNA replication are produced and late phase is when viral DNA

and structural proteins are assembled into virions [46]. Similar to Hawkins *et al.* [12], our mathematical model of EBV infection can be extended to account for these distinct phases of viral infection with corresponding immune response to the phases.

Bibliography

[1] Thorley-Lawson DA. EBV persistence-introducing the virus in Münz C (Ed.) Epstein Barr Virus Volume 1. Curr Top Microbiol Immunol 2015; 390;151-208.

[2] Hutt-Fletcher L. Epstein-Barr virus entry. J Virol 2007; 81:7825-7832.

[3] Sixbey J, Yao Q. Immunoglobulin A-induced shift of Epstein-Barr virus tissue tropism. Science 1992; 255:1578-1580.

[4] Turk S, Jiang R, Chesnokova L, Hutt-Fletcher L. Antibodies to gp350/220 enhance the ability of Epstein-Barr virus to infect epithelial cells. J Virol 2006; 80:9628-9633.

[5] Kurth J, Hansmann ML, Rajewsky K, Kuppers R. Epstein-Barr virus-infected B cells expanding in germinal centers of infectious mononucleosis patients do not participate in the germinal center reaction. Proc Natl Acad Sci USA 2003; 100:4730-4735.

[6] Kurth J, Spicker T, Wustrow J, Strickler GJ, Hansmaan LM, *et al.* EBV-infected B cells in infectious mononucleosis: viral strategies for spreading in the B cell compartment and establishing latency. Immunity 2000; 13:485-495.

[7] Tynell E, Aurelius E, Brandell A, Julander I *et al.* . Acyclovir and prednisolone treatment of acute infectious mononucleosis: a multicenter, double-blind, placebo-controlled study. J Infect Dis. 1996; 174: 324-331.

[8] Luzuriaga K, Sullivan JL. Infectious Mononucleosis. N Engl J Med. 2010; 362: 1993-2000.

[9] Dunmire SK, Hogquist KA, Balfour Jr. HH. Infectious Mononucleosis. Curr Top Microbiol Immunol 2015; 390: 211240.

[10] Giao T Huynh and Frederick R Adler. Alternating host cell tropism shapes persistence, evolution and coexistence of Epstein-Barr virus infections in human. Bull Math Biol 2011; 73; 1754-1773.

[11] Giao T Huynh and Frederick R Adler. Mathematical modeling the age dependence of Epstein-Barr virus associated infectious mononucleosis. Mathematical Medicine and Biology 2012; 29; 245-261.

[12] Jared B Hawkins and Eldgar Delgado-Eckert and David A Thorley-Lawson and Michael Shapiro. The cycle of EBV infection explains persistence, the sizes of the infected cell populations and which come under CTL regulation. PLOS Pathogens 2013; 9(10).

[13] Nemerow GR, Wolfert R, McNaughton ME, Cooper NR. Identification and characterisation of the Epstein-Barr receptor on human B lymphocytes and its relationship to the C3d complement receptor (CR2). J Virol 1985; 55; 347-351.

[14] Fingeroth JD, Weis JJ, Tedder TF, Strominger JL *et al.* . Epstein-Barr virus receptor of human B lymphocytes is the C3d receptor CR2. Proc Natl Acad Sci USA 1984; 81; 4510-4514.

[15] Babckock GJ, Decker LL, Volk M, Thorley-Lawson DA. EBV persistence in memory B cells in vivo. Immunity 1998; 395-404.

[16] Hochberg D, Souza T, Catalina M, Sullivan JL, Luzuriaga K, Thorley-Lawson DA. Acute infection with Epstein-Barr virus targets and overwhelms the peripheral memory B cell compartment with resting, latently infected cells. J Virol 2004; 78(10); 5194-204.

[17] Miyashita EM, Yang B, Babcock GJ, Thorley-Lawson DA. Identification of the siteof Epstein-Barr virus persistence in vivo as a resting B cell. J Virol 1997; 71; 4882-4891.

[18] Hadinoto V, Shapiro M, Sun CC, Thorley-Lawson DA. The dynamics of EBV shedding implicate a central role for epithelial cells in amplifying viral output. PLoS Pathog 2009; 5; e1000496.

[19] Thorley-Lawson DA, Gross A. Persistence of the Epstein-Barr virus and the origins of associated lymphomas. N Engl J Med 2004; 350; 1328-1337.

[20] Thorley-Lawson DA, Allday MJ. The curious case of the tumour virus: 50 years of Burkitt's lymphoma. Nat Rev Microbiol 2008; 6; 913-924.

[21] Gottschalk S, Rooney CM, Heslop HE. Post-transplant lymphoproliferative disorders. Annu Rev Med. 2005; 56: 29-44.

[22] U D Allen and J K Preiksaitis and the AST Infectious Diseases Community of Practice. Epstein-Barr virus and posttransplant lymphoproliferative disorder in solid organ transplantation. Am J Transplant 2013; 13; 107-120.

[23] Green M, Michaels M. Prevention of Epstein-Barr virus infection and posttransplant lymphoproliferative disease following transplantation, in: Dharnidharka VR, Green M, Webber SA (Eds.), Post-transplant lymphoproliferative disorders. Springer, Berlin Heidelberg, 2010.

[24] Olivia L Hatton and Aleishia Harris-Arnold and Steven Schaffert and Sheri M Krams and Olivia M Martinez. The interplay between Epstein-Barr virus and B lymphocytes: implications for infection, immunity, and disease. Immunol Res 2014.

[25] David A Thorley-Lawson. Epstein-Barr virus: exploiting the immune system. Nat Rev Immunol 2001; 1; 75-82.

[26] J L Kutok and F Wang. Spectrum of Epstein-Barr virus-associated dieseases. Annu Rev Pathol Mech Dis 2006; 1; 375-404.

[27] IARC. Epstein-Barr virus. IARC Monogr Eval Carcinog Risks Hum 2012; 100B; 49-92.

[28] Olivia M Martinez. The biology of Epstein-Barr virus and posttransplant lymphoproliferative disease in Vikas R Dharnidharka and Michael Green and Steven A Webber (Eds.), Post-transplant lymphoproliferative disorders. Springer, Berlin Heidelberg 2010.

[29] Helen E Heslop. How I treat EBV lymphoproliferation. Blood 2009; 114(19); 4002-4008.

[30] David A Thorley-Lawson and Jared Hawkins and Sean I Tracy and Michael Shapiro. The pathgenesis of Epstein-Barr virus persistent infection. Curr Opin Virol. 2013; 3; 1-6.

[31] Gerald Bryan Pier and Jeffrey B Lyczak and Lee M Wetzler. Immunology, Infection, and Immunity. ASM Press (1st Ed.) 2004.

[32] Helen E Heslop. How I treat EBV lymphoproliferation. Blood 2009; 114. How I treat. (19); 4002-4008.

[33] Christian Münz. Role of human natural killer cells during Epstein-Barr virus infection. Crit Rev Immunol 2014; 6(34); 501-507.

[34] J E Roughan and C Torgbor and D A Thorley-Lawson. Germinal Center B Cells Latently Infected with Epstein-Barr Virus Proliferate Extensively but Do Not Increase in Number. J Virol 2010; 84(2); 1158-1167.

[35] O A Odumade and K A Hogquist and H H Balfour, Jr. Progress and problems in understanding and managing primary Epstein-Barr visurs infections. Clin Microbiol Rev 2011; 193-209.

[36] Balfour Jr. HH, Odumade OA, Schmeling DO, Mullan BD *et al.* . Behavioral, virologic, and immunologic factors associated with acquisition and severity of primary Epstein-Barr virus infection in university students. J Infect Dis 2013; 207; 80-88.

[37] Peters A, Akinwumi S, Iafolla M, Mabilangan C *et al.* . Epidemiology of post-transplant lymphoproliferative disorders following solid organ transplant in a major Canadian transplant centre. Blood 2013; 122(21); 4281.

[38] Engels EA, Pfeiffer RM, Fraumeni JF, Jr. *et al.* Spectrum of cancer risk among US solid organ transplant recipients. Jama. 2011;306(17):1891-1901.

[39] Peters AC, Akinwumi MS, Cervera C, Mabilanga C *et al.* The changing epidemiology of post-transplant lymphoproliferative disorder in adult solid organ transplant recipients over 30 years: A single centre experience. Manuscript in preparation.

[40] Halloran PF. Immunosuppressive drugs for kidney transplantation. N Engl J Med. 2004 Dec 23; 351(26): 2715–29.

[41] Hardinger KL, Brennan DC, Klein CL. Selection of induction therapy in kidney transplantation. Transpl Int. 2013 Jul;26(7): 671–683.

[42] Khurana A, Brennan DC. Liapis H, Wang HL eds. Current concepts of immunosuppression and side effects. Pathology of Solid Organ Transplantation. 11-30. Springer-Verlad Berlin Heidelberg 2011.

[43] Nemerow GR, Wolfert R, McNaughton ME, Cooper NR. Identification and characterization of the Epstein-Barr virus receptor on human B lymphocytes and its relationship to the C3d complement receptor (CR2). J Virol 1985; 33: 347-351.

[44] Fingeroth JD, Weis JJ, Tedder TF, Strominger JL. *et al.* . Epstein-Barr virus receptor of human B lymphocytes is the C3d receptor CR2. Proc Natl Acad Sci USA 1984; 81: 4510-4514.

[45] Li Q, Spriggs MK, Kovats S, Turk SM *et al.* . Epstein-Barr virus uses HLA class II as a cofactor for infection of B lymphocytes. J Virol 1997; 71: 4657-4662.

[46] Kieff E, Rickinson AB. Epstein-Barr virus and its replication. In: Knipe DM, Howley PM (eds) Fields virology, 5th edn. Lippincontt Williams & Wilkins, Philadelphia.

[47] Thorley-Lawson DA, Strominger JL. Reversible inhibition by phosphonoacetic acid of human B lymphocyte transformation by Epstein-Barr virus. Virology 1978; 86: 423-431.

[48] Nikitin PA, Yan CM, Forte E, Bocedi A *et al.* . An ATM/Chk2-mediated DNA damage-responsive signaling pathway suppresses Epstein-Barr virus transformation of primary human B cells. Cell Host Microbe 2010; 8: 510-522.

[49] Roughan JE, Thorley-Lawson DA. The intersection of Epstein-Barr virus with the germinal center. J Virol 2009; 83: 3968-3976.

[50] Miyashita EM, Yang B, Lam KM, Crawford DH, Thorley-Lawson DA. A novel form of Epstein-Barr virus latency in normal B cells in vivo. Cell 1995; 80: 593-601.

[51] Miyashita EM, Yang B, Babcock GJ, Thorley-Lawson DA. Identification of the site of Epstein-Barr virus persistence in vivo as a resting B cell. J Virol 1997; 71: 4882-4891.

[52] Babcock GJ, Decker LL, Volk M, Thorley-Lawson DA. EBV persistence in memory B cells in vivo. Immunity 1998; 9: 395-404.

[53] Decker LL, Klaman LD, Thorley-Lawson DA. Detection of the latent form of Epstein-Barr virus DNA in the peripheral blood of healthy individuals. J Virol 1996; 70: 3286-3289.

[54] Joseph AM, Babcock GJ, Thorley-Lawson DA. EBV persistence involves strict selection of latently infected B cells. J Immunol 2000; 165: 2975-2981.

[55] Rickinson AB, Moss DJ. Human cytotoxic T lymphocyte responses to Epstein-Barr virus infection. Annu Rev Immunol 1997; 15: 405-31.

[56] Hoffman GJ, Lazarowtiz SE, Hayward SD. Monoclonal antibody against a 250,000-dalton glycoprotein of Epstein-Barr virus identifies a membrane antigen and a neutralising antigen. Proc Natl Acad Sci USA 1980; 77: 2979-83.

[57] Thorley-Lawson DA, Geilinger K. Monoclonal antibodies against the major glycoprotein (gp350/220) of Epstein-Barr virus neutralise infectivity. Proc Natl Acad Sci USA 1980; 77: 5307-11.

[58] Pearson GR, Qualtiere LF, Klein G, Norin T, Bal IS. Epstein-Barr virus-specific antibody-dependent cellular cytotoxicity in patients with Burkitt's lymphoma. Int J Cancer 1979; 24: 402-6.

[59] Craig FE, Gulley ML, Banks PM. Post-transplantation lymphoproliferative disorders. Am J Clin Pathol 1993; 99: 265-76.

[60] Greenspan JS, Greenspan D, Lennette ET, Abrams DI, Conant MA, Petersen V, Freese UK. Replication of Epstein-Barr virus within the epithelial cells of oral "hariy" leukoplakia, an AIDS-associated lesion. N Engl J Med 1985; 313: 1564-71.

[61] Moss DJ, Rickinson AB, Pope JH. Epstein-Barr virus and its relationship to T-cell memory. J Exp Med 1978.

[62] Steven NM, Leese AM, Annels N, Lee S, Rickinson AB. Epitope focusing in the primary cytotoxic T-cell response to Epstein-Barr virus and its relationship to T-cell memory. J Exp Med 1996.

[63] Hsu D-H, de Waal Malefyt R, Fiorentino DF, Dang M-N, Vieira P, de Vries J, Spits H, Hosmann TR, Moore KW. Expression of interleukin-10 activity by Epstein-Barr virus protein BCRF1. Science 1990; 250: 830-32.

[64] Vieira P, de Waal-Malefyt R, Dang MN, Johnson KE, Kastelein R, Fiorentino DF, de Vries JE, Roncarolo MG, Mosmann TR, Moore KW. Isolation and expression of human cytokine synthesis inhibitory factor cDNA clones: homology to Epstein-Barr virus open reading frame BCRF1. Proc Natl Acad Sci USA 1991; 88: 1172-76.

[65] Rousset F, Garcia E, Defrance T, Peronne C, Vezzio N, Hsu DH, Kastelein R, Moore KW, Banchereau J. Interleukin 10 is a potent growth and differentiation factor for activated human B lymphocytes. Proc Natl Acad Sci USA 1992; 89: 1890-93.

[66] Stuart AD, Stewart JP, Arrand JR, Mackett M. The Epstein-Barr virus encoded cytokine viral interleukin-10 enhances transformation of human B lymphocytes. Oncogene 1995; 11: 1711-19.

[67] Suzuki T, Tahara H, Narula S, Moore KW, Robbins RD, Lotze MT. Viral interleukin 10 (IL-10), the human herpesvirus 4 cellular IL-10 homologue, induces local anergy to allogeneic and syngeneic tumours. J Exp Med 1995; 182: 477-86.

[68] Hislop AD, Taylor GS, Sauce D, Rickinson AB. Cellular responses to viral infection in humans: lessons from Epstein-Barr virus. Annu Rev Immunol 2007; 25: 587-617.

[69] Odumade OA, Knight JA, Schmeling DO, Masopust D, Balfour Jr. HH, Hogquist KA. Primary Epstein-Barr virus infection does not erode pre-existing $CD8^+$ T cell memory in humans. J Exp Med 2012; 209: 471-478.

[70] Eidenschenk C, Dunne J, Jouanguy E, Fourlinnie C, Gineau L, Bacq D, McMahon C, Smith O, Casanova JL, Abel L, Feighery C. A novel primary immunodeficiency with specific natural-killer cell deficiency maps to the centromeric region of chromosome 8. Am J Hum Genet 2006; 78: 721-727.

[71] Parolini S, Bottino C, Falco M, Augugliaro R, Giliani S, Franceschini R, Ochs HD, Wolf H, Bonnefoy JY, Biassoni R *et al.* . X-linked lymphoproliferative disease. 2B4 molecules displaying inhibitory rather than activating function are responsible for the inhability of natural killer cells to kill Epstein-Barr virus-infected cells. J Exp Med 2000; 192: 337-346.

[72] Shaw RK, Issekutz AC, Fraser R, Schmit P, Morash B, Monaco-Shawver L, Orange JS, Fernandez CV. Bilateral adrenal EBV-associated smooth muscle tumors in a child with a natural killer cell deficiency. Blood 2012; 119: 4009-4012.

[73] Williams H, McAulay K, Macsween KF, Gallacher NJ, Higgins CD, Harrison N, Swerdlow AJ, Crawford DH. The immune response to primary EBV infection: a role for natural killer cells. Br J Haematol 2005; 129: 266-274.

[74] Chijioke O, Müller A, Feederie R, Barros MH, Krieg C, Emmel V, Marcenaro E, Leung CS, *et al.* . Human natural killer cells prevent infectious mononucleosis features by targeting lytic Epstein-Barr virus infection. Cell Reports 2013; 5: 1489-1498.

[75] Gottschalk S, Rooney CM, Heslop HE. Post-transplant lymphoproliferative disorders. Annu Rev Med. 2005; 56: 29-44.

[76] U D Allen and J K Preiksaitis and the AST Infectious Diseases Community of Practice. Epstein-Barr virus and posttransplant lymphoproliferative disorder in solid organ transplantation. Am J Transplant 2013; 13; 107-120.

[77] Green M, Michaels M. Prevention of Epstein-Barr virus infection and posttransplant lymphoproliferative disease following transplantation, in: Dharnidharka VR, Green M, Webber SA (Eds.), Post-transplant lymphoproliferative disorders. Springer, Berlin Heidelberg, 2010.

[78] Olivia L Hatton and Aleishia Harris-Arnold and Steven Schaffert and Sheri M Krams and Olivia M Martinez. The interplay between Epstein-Barr virus and B lymphocytes: implications for infection, immunity, and disease. Immunol Res 2014.

[79] David A Thorley-Lawson. Epstein-Barr virus: exploiting the immune system. Nat Rev Immunol 2001; 1; 75-82.

[80] J L Kutok and F Wang. Spectrum of Epstein-Barr virus-associated dieseases. Annu Rev Pathol Mech Dis 2006; 1; 375-404.

[81] David A Thorley-Lawson and Andrew Gross. Persistence of the Epstein-Barr virus and the origins of associated lymphomas. N Engl J Med 2004; 350; 1328-37.

[82] IARC. Epstein-Barr virus. IARC Monogr Eval Carcinog Risks Hum 2012; 100B; 49-92.

[83] Olivia M Martinez. The biology of Epstein-Barr virus and posttransplant lymphoproliferative disease in Vikas R Dharnidharka and Michael Green and Steven A Webber (Eds.), Post-transplant lymphoproliferative disorders. Springer, Berlin Heidelberg 2010.

[84] Jianyong Wu and Radhika Dhingra and Manoj Gambhir and Justin V Remais. Sensitivity analysis of infectious disease models: methods, advances and their application. J R Soc Interface 2013; 10(86); 10.1098/rsif.2012.1018.

[85] Helen E Heslop. How I treat EBV lymphoproliferation. Blood 2009; 114(19); 4002-4008.

[86] Vey Hadinoto and Michael Shapiro and Thomas C Greenough and John L Sullivan and Katherine Luzuriaga and David A Thorley-Lawson. On the dynamics of acute EBV infection and the pathogenesis of infectious mononucleosis. Blood 2008; 111(3); 1419-1427.

[87] David A Thorley-Lawson and Jared Hawkins and Sean I Tracy and Michael Shapiro. The pathgenesis of Epstein-Barr virus persistent infection. Curr Opin Virol. 2013; 3; 1-6.

[88] M Shapiro and K A Duca and K Lee and E Delgado-Eckert and J Hawkins and A S Jarrah and R Laubenbacher and N F Polys and V Hadinoto and D A Thorley-Lawson. A virtual look at Epstein-Barr virus infection: Simulation Mechanism. J Theor Biology 2008; 252(4); 633-648.

[89] Giao T Huynh and Frederick R Adler. Alternating host cell tropism shapes persistence, evolution and coexistence of Epstein-Barr virus infections in human. Bull Math Biol 2011; 73; 1754-1773.

[90] Jared B Hawkins and Eldgar Delgado-Eckert and David A Thorley-Lawson and Michael Shapiro. The cycle of EBV infection explains persistence, the sizes of the infected cell populations and which come under CTL regulation. PLOS Pathogens 2013; 9(10).

[91] John Lang and Michael Y Li. Stable and transient periodic oscillations in a mathematical model for CTL response to HTLV-I infection. J Math Biol 2012; 65; 181-199.

[92] Gerald Bryan Pier and Jeffrey B Lyczak and Lee M Wetzler. Immunology, Infection, and Immunity. ASM Press (1st Ed.) 2004.

[93] Dominik Wodarz and Martin A Nowak and Charles R M Bangham. The dynamics of HTLV-1 and the CTL response. Immunol Today 1999; 20; 220-227.

[94] Martin A Nowak and Robert M May. Virus dynamics: mathematical principles of immunology and virology. Oxford University Press, Oxford 2000.

[95] Yo Hoshino and Harutaka Katano and Ping Zou and Patricia Hohman and Adriana Marques and Stephen K Tyring and Dean Follman and Jeffrey I Cohen. Long-term administration of valganciclovir reduces the number of Epstein-Barr virus (EBV)-infected B cells but not the number of EBV DNA copies per B cell in healthy volunteers. J Virol 2009; 83(22); 11857-11861.

[96] Thomas Matthews and Richard Boehne. Antiviral activity and mechanism of action of Ganciclovir. Rev Infect Dis 1988; 10, Supplement 3. Cytomegalovirus Infection and Treatment with Ganciclovir; S490-S494.

[97] Nicholas H G Holford and Lewis B Sheiner. Kinetics of pharmacology response. Pharmac Ther 1982; 16; 143-166.

[98] David W A Bourne. Pharmacokinetic models in Mathematical modeling of pharmacokinetic data. Technomic Publishing Company, Inc. Lancaster, Pennsylvania 1995.

[99] Helen E Heslop. How I treat EBV lymphoproliferation. Blood 2009; 114. How I treat. (19); 4002-4008.

[100] Sunil S Jambhekar and Philip J Breen. Extravascular routes of drug administration in Basic pharmacokinetics. Pharmaceutical Press; London, UK 2012 (2nd ed.)

[101] Anthea Peters and Segun Akinwumi and Marco Iafolla and Curtis Mabilangan and Karen Doucette and Jutta Preiksaitis Epidemiology of post-transplant lymphoproliferative disorders following solid organ transplant in a major Canadian transplant centre. Blood 2013; 122(21); 4281.

[102] Christian Münz. Role of human natural killer cells during Epstein-Barr virus infection. Crit Rev Immunol 2014; 6(34); 501-507.

[103] S M Blower and H Dowlatabadi. Sensitivity and uncertainty analysis of complex models of disease transmissions: an HIV model, as an example. Int Stat Rev 1994; 62(2); 229-243.

[104] Simeone Marino and Ian B Hogue and Christian J Ray and Denise E Kirschner. A methodology for performing global uncertainty and sensitivity analysis in systems biology. J Theor Biol 2008; 254(1); 178-196.

[105] O A Odumade and K A Hogquist and H H Balfour, Jr. Progress and problems in understanding and managing primary Epstein-Barr visurs infections. Clin Microbiol Rev 2011; 193-209.

[106] H H Balfour, Jr. and O A Odumade and D O Schmeling and B D Mullan and J A Ed and J A Knight and H E Vezina and W Thomas and K A Hogquist. Behavioral, virologic, and immunologic factors associated with acquisition and severity of primary Epstein-Barr virus infection in university students. J Infect Dis 2013; 207; 80-88.

[107] S Fafi-Kremer and P Morand and J Brion and P Parese and M Baccard and R Germi and O Genoulaz and S Nicod and M Jolivet and R W H Ruigrok and J Stahl and J Seigneurin. Long-term shedding of infectious Epstein-Barr virus after infectious mononucleosis. J Infect Dis 2005; 191; 985-989.

[108] J E Roughan and C Torgbor and D A Thorley-Lawson. Germinal Center B Cells Latently Infected with Epstein-Barr Virus Proliferate Extensively but Do Not Increase in Number. J Virol 2010; 84(2); 1158-1167.

[109] E Delgado-Eckert and M Shapiro. A model of host response to a multi-stage pathogen. J Math Biol 2010; 63(2); 201-227.

[110] O Diekmann and J A P Heesterbeek and M G Roberts. The construction of next-generation matrices for compartmental epidemic models. J R Soc Interface 2010; 7(47); 873-885.

[111] P van den Driessche and J Watmough. Reproduction numbers and sub-threshold endemic equilibria for compartmental models of disease transmission. Mathematical Biosciences 2002; 180(1-2); 29-48.

[112] B Efron and R Tibshirani. Bootstrap methods for standard errors, confidence intervals, and other measures of statistical accuracy. Statist Sci 1986; 1(1); 54-75.

[113] Thorley-Lawson DA, Gross A. Persistence of the Epstein-Barr virus and the origins of associated lymphomas. N Engl J Med. 2004 Mar 25; 350(13): 1328–37.

[114] Thorley-Lawson DA. Epstein-Barr virus: exploiting the immune system. Nat Rev Immunol. 2001; 1(1): 75–82.

[115] Thorley-Lawson DA, Hawkins J, Tracy SI, Shapiro M. The pathogenesis of Epstein-Barr virus persistent infection. Curr Opinion Virol. 2013; 3(3): 227–32.

[116] Akinwumi MS, Li MY, Preiksaitis J. Modeling the kinetics of primary EBV infection with implications for viral persistence and disease management. Manuscript in preparation.

[117] Halloran PF. Immunosuppressive drugs for kidney transplantation. N Engl J Med. 2004 Dec 23; 351(26): 2715–29.

[118] Hardinger KL, Brennan DC, Klein CL. Selection of induction therapy in kidney transplantation. Transpl Int. 2013 Jul;26(7): 671–683.

[119] Gurkan S, Luan Y, Dhillon N, et al. Immune reconstitution following rabbit antithymocyte globulin. Am J Transplant. 2010 Sep; 10(9): 2132–41.

[120] Wagner SJ, Brennan DC. Induction therapy in renal transplant recipients. Drugs. 2012;72(5): 75–82.

[121] Golay J, Semenzato G, Rambaldi A, et al. Lessons for the clinic from rituximab pharmacokinetics and pharmacodynamics. MAbs. 2013 Nov-Dec; 5(6): 826–37.

[122] Pescovitz MD. Rituximab, an anti-CD20 monoclonal antibody: history and mechanism of action. Am J Transplant. 2006 May; 6(5 Pt 1): 859–866.

[123] Kahwaji J, Tong C, Jordan SC, Vo AA. Rituximab: An emerging therapeutic agent for kidney transplantation. Transplant Research and Risk Management. 2009 Oct; 2009(1): 15–29.

[124] Bourne DWA. Mathematical modeling of pharmacokinetic data. Technomic Publishing Company, Lancaster, PA: Technomic Publishing AG.; 1995.

[125] Hröcker B, Bröhm S, Fickenscher H, et al. (Val-)Ganciclovir prophylaxis reduces Epstein-Barr virus primary infection in pediatric renal transplantation. Transpl Int. 2012; 25(7): 723-731.

[126] Matthews T, Boehme R. Antiviral activity and mechanism of action of Ganciclovir. Rev. Infect. Dis.; 1988; 10(3); S490-S494.

[127] Venturi C, Bueno J, Gavalda J, et al. Impact of Valganciclovir on Epstein-Bein virus polymerase chain reaction in pediatric liver transplantation: preliminary report. Transplant Proc. 2009 Apr; 41(3): 1038-40.

[128] Ramirez CB, Bozdin A, Frank A, et al. Optimizing use of basiliximab in liver transplantation. Transplant Research and Risk Management. 2010 Oct; 2: 1-10.

[129] Mohty M Mechanisms of action of antithymocyte globulin: T-cell depletion and beyond. Leukemia. 2007; 21: 1387-1394.

[130] Duhart Jr. BT, Ally WA, Krauss AG, et al. The benefit of sirolimus maintenance immunosuppression and rabbit antithymocyte globulin induction in liver transplant recipients that develop acute kidney injury

in the early postoperative period. Journal of Transplantation, vol. 2015, Article ID 926168, 6 pages, 2015. doi:10.1155/2015/926168.

[131] Khurana A, Brennan DC. Liapis H, Wang HL eds. Current concepts of immunosuppression and side effects. Pathology of Solid Organ Transplantation. 11-30. Springer-Verlad Berlin Heidelberg 2011.

[132] Koizumi Y, Iwami S Mathematical modeling of multi-drugs therapy: a challenge for determining the optimal combinations of antiviral drugs. Theor Biol Med Model, vol. 11: 41, 2014. doi:10.1186/1742-4682-11-41.

[133] Dhillon S, Kostrzewski AJ eds Clinical Pharmacokinetics. London, UK: Pharmaceutical Press; 2006. 1st ed.

[134] Gallon LG, Winoto J, Leventhal JR, et al. Effect of prednisone versus no prednisone as part of maintenance immunosuppression on long-term renal transplant function. Clin J Am Soc Nephrol 1: 1029 - 1038, 2006. doi:10.2215/CJN.00790306.

[135] Gurkan S, Schröppel B, Murphy B. Liapis H, Wang HL eds. Immunology of organ transplantation. Pathology of Solid Organ Transplantation. 3-10. Springer-Verlad Berlin Heidelberg 2011.

[136] Hadinoto V, Shapiro M, Greenough T, et al. On the dynamics of acute EBV infection and the pathogenesis of infectious mononucleosis. Blood vol. 111:3, 1419-7, 2008.

[137] Shapiro M, Duca KA, Lee K, et al. A virtual look at Epstein-Barr virus infection: Simulation Mechanism. J Theor Biology 252:3, 633-648, 2008.

[138] Hoshino Y, Katano H, Zou P, et al. Long-term administration of valganciclovir reduces the number of Epstein-Barr virus (EBV)-infected B cells but not the number of EBV DNA copies per B cell in healthy volunteers. J Virol 83:22, 11857-11861, 2009.

[139] Vezina HE, Brundage RC, Balfour Jr HH. Population pharmacokinetics of valganciclovir prophylaxis in paediatric and adult solid organ transplant recipients. Br J Clin Pharmacol 78:2, 343-352, 2014.

[140] Sugiyama K, Isogai K, et al. Comparative study of the cellular pharmacodynamics of tacrolimus in renal transplant recipients treated with and without basiliximab. Cell Transplantation, Vol 21, pp 565-570, 2012.

[141] Vadcharavivad S, Praisuwan S, et al. Population pharmacokinetics of tacrolimus in Thai kidney transplant patients: comparison with similar data from other populations. Journal of Clinical Pharmacy and Therapeutics, Vol 41, pp 310-328, 2016.

[142] Staatz CE, Tett SE Clinical pharmacokinetics and pharmacodynamics of mycophenolate in solid organ transplant recipients. Clin Pharmacokinetic 46(1), pp 13-58, 2007.

[143] Teeninga N, Guan Z, et al. Population pharmacokinetics of prednisolone in relation to clinical outcome in children with nephrotic syndrome. The Drug Monit 38(4), pp 534-545, 2016.

[144] Admiraal R, van Kesteren C, et al. Population pharmacokinetic modeling of thymoglobulin in children receiving allogeneic-hematopoietic cell transplantation: towards improved survival through individualised dozing. Clin Pharmacokinetic 54, pp 435-446, 2015.

[145] Ayuk F, Perez-Simon JA, et al. Clinical impact of human jurkat T-cell-line-derived antithymocyte globulin in multiple myeloma patients undergoing allogeneic stem cell transplantation. Haematologica 93(9), pp 1343-1350, 2008.

[146] Puisset F, White-Koning M, et al. Population pharmacokinetics of rituximab with or without plasmapheresis in kidney patients with antibody-mediated disease. Br J Clin Pharmacol 76:5, 734-740, 2014.

[147] Enderby C, Keller CA An overview of immunosuppression in solid organ transplantation. Am J Manag Care. 2015; 21: S12–S23.

[148] Allen UD, Preiksaitis JK, the AST Infectious Diseases Community of Practice Epstein-Barr virus and posttransplant lymphoproliferative disorder in solid organ transplantation. Am J Transplant. 2013; 13: 107–120.

[149] Allen UD, Preiksaitis JK, the AST Infectious Diseases Community of Practice Epstein-Barr virus and posttransplant lymphoproliferative disorder in solid organ transplant recipients. Am J Transplant. 2009; 9 (Suppl 4): S87S96.

[150] Jayasooriya S, de Silva TI, Njie-jobe J et al. Early virological and immunological events in asymptomatic Epstein-Barr Virus infection in African children. PLOS Pathogens. 2015; 11(3): e1004746.

[151] Wagner SJ, Brennan DC Induction therapy in renal transplant recipients, how convincing is the current evidence?. Drugs 2012: 72(5): 671-683.

[152] Chong AS, Alegre M The impact of infection and tissue damage in solid-organ transplantation. Nat Rev Immunol. 2012 May 25;12(6):459-71.

[153] Martin-Gandul C, Mueller NJ, et al. The impact of infection on chronic allograft dysfunction and allograft survival after solid organ transplantation. American Journal of Transplantation 2015; 15: 30243040.

[154] Dalal P, Shah G, et al. Role of tacrolimus combination therapy with mycophenolate mofetil in the prevention of organ rejection in kidney transplant patients. International Journal of Nephrology and Renovascular Disease 2010; 3: 107–115.

[155] Bouvy AP, Kho MML, et al. Kinetics of homeostatic proliferation and thymopoiesis after rATG induction therapy in kidney transplant recipients. Transplantation. 2013 Nov 27; 96(10): 94–13.

[156] Blower SM, Dowlatabadi H Sensitivity and uncertainty analysis of complex models of disease transmissions: an HIV model, as an example. Int Stat Rev 1994; 62; 229-243.

[157] Marino S, Hogue IB, et al. A methodology for performing global uncertainty and sensitivity analysis in systems biology. J Theor Biol 2008; 254: 178-196.

[158] Wu J, Dhingra R, et al. Sensitivity analysis of infectious disease models: methods, advances and their application. J R Soc Interface 2013; 10;.

[159] Krepsova E, Tycova I, et al. Effect of induction therapy on the expression of molecular markers associated with rejection and tolerance. BMC Nephrology 2015; 16:146.

[160] Bücher M, Longuet H, et al. Pharmacokinetic and pharmacodynamic studies of two different rabbit antithymocyte globulin dosing regimens: Results of a randomized trial. Transplant Immunology 2013; 28: 120-126.

[161] Wu J, Dhingra R, et al. Regulatory T cells and T cell depletion: Role of immunosuppressive drugs. J Am Soc Nephrol 2007; 18; 1007-1018.

[162] MathWorks MATLAB, R2015b The MathWorks Inc., Natick, MA, USA

[163] Leandro MJ B-cell subpopulations in humans and their differential susceptibility to depletion with anti-CD20 monoclonal antibodies. Arthritis Rsearch & Therapy 2013; 15(Suppl 1):S3.

[164] Sidner BA, Book BK, et al. *In vivo* human B-cell subset recovery after *in vivo* depletion with rituximab, anti-human CD20 monoclonal antibody. Human Antibodies 2004; 13: 55-62.

[165] Maloney DG, Liles TM, et al. Phase I clinical trial using escalating single-dose infusion of chimeric anti-CD20 monoclonal antibody (IDEC-C2B8) in patients with recurrent B-cell lymphoma. Blood 1994; 84: 2457-2466.

[166] Maloney DG, Grillo-Lopez AJ, et al. IDEC-C2B8 (Rituximab) anti-CD20 monoclonal antibody therapy in patients with relapsed low-grade non-Hodgkin's lymphoma. Blood 1997; 90(6): 2188-2195.

[167] McLaughlin P, Grillo-Lopez A, et al. Rituximab chimeric anti-CD20 monoclonal antibody therapy for relapsed indolent lymphoma: half of patients respond to a four-dose treatment program. J Clin Oncol 1998; 16: 2825-2833.

Appendices

Appendix A

Derivation of Basic Reproduction Number for Equations 2.1–2.9

We derived the basic reproduction number R_0 for equations 2.1–2.9 using the next generation matrix number method [110, 111].

Equations 2.1–2.6 constitute the infected susbsystem for our model and Vector $x_0 = (0, \frac{\lambda_n}{\delta_n}, 0, 0, 0, 0)$ is its disease-free equilibrium. In this subsystem, let $F_i(\bar{x})$ denote the rate of appearance of new infections in compartment i and let $V_i(\bar{x}) = V_i^-(\bar{x}) - V_i^+(\bar{x})$, where $V_i^+(\bar{x})$ is the rate of transfer into compartment i by all other means and $V_i^-(\bar{x})$ is the rate of transfer of individuals out of the ith compartment.

The next generation matrix (operator) FV^{-1} from matrices of partial derivatives of F_i and V_i evaluated at x_0 for the infected subsystem is given by

$$FV^{-1}(x_0) = \begin{bmatrix} 0 & 0 & 0 & 0 & n\delta_l \\ (1-\beta)\mu_e\frac{\lambda_n}{\delta_n} & 0 & 0 & 0 & 0 \\ 0 & 0 & 0 & 0 & 0 \\ 0 & 0 & 0 & 0 & 0 \\ 0 & 0 & 0 & 0 & 0 \end{bmatrix} \times$$

$$\begin{bmatrix} \delta_e & 0 & 0 & 0 & n\delta_l \\ 0 & -(r_g - \omega_g - \delta_g) & 0 & 0 & 0 \\ 0 & -\omega_g & -(r_d - \omega_d - \delta_d) & 0 & 0 \\ 0 & 0 & -\omega_d & -(r_m - \omega_m - \delta_m) & 0 \\ 0 & 0 & 0 & -\omega_m & \delta_l \end{bmatrix}^{-1} \tag{1.1}$$

The spectral radius of matrix $FV^{-1}(x_0)$ is the basic reproduction number R_0 which we derived to be

$$R_0 = \frac{n(1-\beta)\mu_e\lambda_n\omega_g\omega_d\omega_m}{\delta_e\delta_n(w_g+\delta_g-r_g)(w_d+\delta_d-r_d)(w_m+\delta_m-r_m)}, \text{ where } R_0 > 0. \quad (1.2)$$

Appendix B

MATLAB functions used for simulation

B.1 MATLAB functions for chapter 2

```
% PTLD project
% ODE file for EBV
% Created by: Michael Akinwumi
% Last modified: Mar 25, 2015
function [dx]=ebvodeNew1(t,x,p)
%Parameters
    global t0
    global td
    rG=p(1);
    omegaG=p(2);
    rD=p(3);
%     alpha2=p(4);
    omegaM = p(4);
    deltaL=p(5);
    n=p(6);
    deltaE=p(7);
    lambdaN=p(8);
    beta=p(9);
    muE=p(10);
    deltaN=p(11);
    deltaG=p(12);
    delta1=p(13);
    deltaD=p(14);
    omegaD=p(15);
```

```
25        delta2=p(16);
26        deltaM=p(17);
27        delta3=p(18);
28        r1=p(19);
29        r2=p(20);
30        r3=p(21);
31        rM=p(22);
32        d1=p(23);
33        d2=p(24);
34        d3=p(25);
35  %       alpha1 = p(26);
36  %       alpha3 = p(27);
37        c = p(26);
38  %%State variables
39        E=x(1);
40        Bn=x(2);
41        Bg=x(3);
42        Bd=x(4);
43        Bm=x(5);
44        Bl=x(6);
45        T1=x(7);
46        T2=x(8);
47        T3=x(9);
48  %%ODEs
49        dx=zeros(9,1);
50  %       dx(1)=n*deltaL*Bl-deltaE*E;%EBV
51  %           dx(1)=(n+n*c*(heaviside(t-t0-td)-heaviside(t-
        t0)))*deltaL*Bl-deltaE*E;%EBV short term treatment
52            dx(1)= (n + n*(c-1)*heaviside(t-t0) + n*(1-c)*
                  heaviside(t-td))*deltaL*Bl-deltaE*E;%EBV long
                    term treatment
53        dx(2)=lambdaN-muE*E*Bn-deltaN*Bn;%Naive B cells
54        dx(3)=(1-beta)*muE*E*Bn+(rG-omegaG-deltaG)*Bg-delta1
             *T1*Bg;%Growth B cells
55        dx(4)=omegaG*Bg+(rD-deltaD-omegaD)*Bd-delta2*T2*Bd;%
             GC B cells
56  %       dx(5)=omegaD*Bd+((1 + alpha3)*rM-alpha2-deltaM)*Bm
        ;%Memory B cells
57  %       dx(6)=((1-alpha1)*deltaM + alpha2 + (1-alpha3)*rM)
        *Bm-deltaL*Bl-delta3*T3*Bl;%Lytic B cells
58        dx(5)=omegaD*Bd+(rM-omegaM-deltaM)*Bm;%Memory B
```

```
        cells
59      dx(6)=omegaM*Bm-deltaL*Bl-delta3*T3*Bl;%Lytic B
        cells
60      dx(7)=r1*T1*Bg-d1*T1;%CTL response to Bg
61      dx(8)=r2*T2*Bd-d2*T2;%CTL response to Bd
62      dx(9)=r3*T3*Bl-d3*T3;%CTL response to Bl
```

```
1  % PTLD project
2  % ODE file for EBV
3  % Created by: Segun Akinwumi
4  % Last modified: Jan 7, 2014
5  function [dx]=ebvodeNew2(t,x,p)
6  %Parameters
7  rG=p(1);
8  omegaG=p(2);
9  rD=p(3);
10 omegaM=p(4);
11 deltaL=p(5);
12 n=p(6);
13 deltaE=p(7);
14 lambdaN=p(8);
15 beta=p(9);
16 muE=p(10);
17 deltaN=p(11);
18 deltaG=p(12);
19 delta1=p(13);
20 deltaD=p(14);
21 omegaD=p(15);
22 delta2=p(16);
23 deltaM=p(17);
24 delta3=p(18);
25 r1=p(19);
26 r2=p(20);
27 r3=p(21);
28 rM=p(22);
29 d1=p(23);
30 d2=p(24);
31 d3=p(25);
32 %State variables
33 E=x(1);
34 Bn=x(2);
```

```
Bg=x(3);
Bd=x(4);
Bm=x(5);
Bl=x(6);
T1=x(7);
T2=x(8);
T3=x(9);
%ODEs
dx=zeros(9,1);
dx(1)=n*deltaL*Bl-deltaE*E;%EBV
dx(2)=lambdaN-(1-beta)*muE*E*Bn-deltaN*Bn;%Naive B cells
dx(3)=(1-beta)*muE*E*Bn+(rG-omegaG-deltaG)*Bg-delta1*T1*
    Bg;%Growth B cells
dx(4)=omegaG*Bg+(rD-deltaD-omegaD)*Bd-delta2*T2*Bd;%GC B
     cells
dx(5)=omegaD*Bd+(rM-omegaM-deltaM)*Bm;%Memory B cells
dx(6)=omegaM*Bm-deltaL*Bl-delta3*T3*Bl;%Lytic B cells
dx(7)=r1*T1/(T1+2)*Bg-d1*T1;%CTL response to Bg
dx(8)=r2*T2/(T2+2)*Bd-d2*T2;%CTL response to Bd
dx(9)=r3*T3/(T3+2)*Bl-d3*T3;%CTL response to Bl
```

B.2 MATLAB functions for chapter 3

B.2.1 Maintenance immunosuppression and antithymocyte globulin

```
% PTLD project
% ODE file for EBV
% Created by: Michael Akinwumi
% Last modified: Jan 31, 2017
function [dx] = maintenanceATG(t,x,p)
%Parameters
    rG=p(1); omegaG=p(2); rD=p(3); omegaM = p(4); deltaL
       =p(5); n=p(6); deltaE=p(7); lambdaN=p(8); beta=p
       (9); muE=p(10);
    deltaN=p(11); deltaG=p(12); delta1=p(13); deltaD=p
       (14); omegaD=p(15); delta2=p(16); deltaM=p(17);
       delta3=p(18); r1=p(19); r2=p(20);
    r3=p(21); rM=p(22); d1=p(23); d2=p(24); d3=p(25);
%Maintenance Immunosuppression and ATG
    emax = p(26); t01 = p(27); t11 = p(28); emin = p(29)
       ;
```

```
12      amax = p(30); t02 = p(31); t12 = p(32); amid = p(33)
            ; amin = p(34);
13      eM = emax + (emin-emax)/(t11-t01)*(t-t01)*heaviside(
            t-t01) + (emin - (emax + (emin-emax)/(t11-t01)*(t
            -t01)))*heaviside(t-t11);
14      eA = amax-(amax-amin)/t02*t + (amin+(amid-amin)/(t12
            -t02)*(t-t02)-(amax-(amax-amin)/t02*t)).*
            heaviside(t-t02) + ...
15            (amid - (amin+(amid-amin)/(t12-t02)*(t-t02))).*
                heaviside(t-t12) ;
16  %State variables
17      E=x(1); Bn=x(2); Bg=x(3); Bd=x(4); Bm=x(5); Bl=x(6);
            T1=x(7); T2=x(8); T3=x(9);
18  %%ODEs
19      dx=zeros(9,1);
20      dx(1)=n*deltaL*Bl-deltaE*E;%EBV
21      dx(2)=lambdaN-muE*E*Bn-deltaN*Bn;%Naive B cells
22      dx(3)=(1-beta*(1-eA))*muE*E*Bn+(rG-omegaG-deltaG)*Bg
            -delta1*T1*Bg;%Growth B cells *(1-eA)
23      dx(4)=omegaG*Bg+(rD-deltaD-omegaD)*Bd-delta2*T2*Bd;%
            GC B cells
24      dx(5)=omegaD*Bd+(rM-omegaM-deltaM)*Bm;%Memory B
            cells
25      dx(6)=omegaM*Bm-deltaL*Bl-delta3*T3*Bl;%Lytic B
            cells
26      dx(7)=(1-eM)*r1*T1*Bg-d1*T1-(1-eA)*T1;%CTL response
            to Bg
27      dx(8)=(1-eM)*r2*T2*Bd-d2*T2-(1-eA)*T2;%CTL response
            to Bd
28      dx(9)=(1-eM)*r3*T3*Bl-d3*T3-(1-eA)*T3;%CTL response
            to Bl
```

B.2.2 Maintenance immunosuppression, antithymocyte globulin and valganciclovir

```
1  % PTLD project
2  % ODE file for EBV
3  % Created by: Michael Akinwumi
4  % Last modified: Jan 31, 2017
5  function [dx] = maintenanceATGAntiviral(t,x,p)
6  %Parameters
```

```
7       rG=p(1); omegaG=p(2); rD=p(3); omegaM = p(4); deltaL
            =p(5); n=p(6); deltaE=p(7); lambdaN=p(8); beta=p
            (9); muE=p(10);
8       deltaN=p(11); deltaG=p(12); delta1=p(13); deltaD=p
            (14); omegaD=p(15); delta2=p(16); deltaM=p(17);
            delta3=p(18); r1=p(19); r2=p(20);
9       r3=p(21); rM=p(22); d1=p(23); d2=p(24); d3=p(25);
10  %Maintenance Immunosuppression and ATG
11      emax = p(26); t01 = p(27); t11 = p(28); emin = p(29)
            ;
12      amax = p(30); t02 = p(31); t12 = p(32); amid = p(33)
            ; amin = p(34);
13      eM = emax + (emin-emax)/(t11-t01)*(t-t01)*heaviside(
            t-t01) + (emin - (emax + (emin-emax)/(t11-t01)*(t
            -t01)))*heaviside(t-t11);
14      eA = amax-(amax-amin)/t02*t + (amin+(amid-amin)/(t12
            -t02)*(t-t02)-(amax-(amax-amin)/t02*t)).*
            heaviside(t-t02) + ...
15          (amid - (amin+(amid-amin)/(t12-t02)*(t-t02))).*
                heaviside(t-t12) ;
16  %Valganciclovir
17      DV = p(35); VV = p(36); ka = p(37); kel = p(38);
            tauV = p(39); ICV = p(40); epV = p(41); tstart =
            p(42); tend = p(43);
18      nV = heaviside(t-tstart)*(1 + floor((t-tstart)/tauV)
            );
19      CV = DV/VV*ka/(ka-kel)*((1-exp(-nV*kel*tauV))/(1-exp
            (-kel*tauV))*exp(-kel*mod(t,tauV)) - (1-exp(-nV*
            ka*tauV))/(1-exp(-ka*tauV))*exp(-ka*mod(t,tauV)))
            ;
20      eV = epV*CV/(CV + ICV)*heaviside(t-(tstart+2)) - epV
            *CV/(CV + ICV)*heaviside(t-tend);
21  %State variables
22      E=x(1); Bn=x(2); Bg=x(3); Bd=x(4); Bm=x(5); Bl=x(6);
             T1=x(7); T2=x(8); T3=x(9);
23  %%ODEs
24      dx=zeros(9,1);
25      dx(1)=(1-eV/.7)*n*deltaL*Bl-deltaE*E;%EBV
26      dx(2)=lambdaN-muE*E*Bn-deltaN*Bn;%Naive B cells
27      dx(3)=(1-beta*(1-eA))*muE*E*Bn+(rG-omegaG-deltaG)*Bg
            -delta1*T1*Bg;%Growth B cells *(1-eA)
```

```
28      dx(4)=omegaG*Bg+(rD-deltaD-omegaD)*Bd-delta2*T2*Bd;%
            GC B cells
29      dx(5)=omegaD*Bd+(rM-omegaM-deltaM)*Bm;%Memory B
            cells
30      dx(6)=omegaM*Bm-deltaL*Bl-delta3*T3*Bl;%Lytic B
            cells
31      dx(7)=(1-eM)*r1*T1*Bg-d1*T1-(1-eA)*T1;%CTL response
            to Bg
32      dx(8)=(1-eM)*r2*T2*Bd-d2*T2-(1-eA)*T2;%CTL response
            to Bd
33      dx(9)=(1-eM)*r3*T3*Bl-d3*T3-(1-eA)*T3;%CTL response
            to Bl
```

B.2.3 Maintenance immunosuppression, antithymocyte globulin and rituximab

```
1  % PTLD project
2  % ODE file for EBV
3  % Created by: Michael Akinwumi
4  % Last modified: Jan 31, 2017
5  function [dx] = maintenanceATGRituximab(t,x,p,q)
6  %Parameters
7       rG=p(1); omegaG=p(2); rD=p(3); omegaM = p(4); deltaL
            =p(5); n=p(6); deltaE=p(7); lambdaN=p(8); beta=p
            (9); muE=p(10);
8       deltaN=p(11); deltaG=p(12); delta1=p(13); deltaD=p
            (14); omegaD=p(15); delta2=p(16); deltaM=p(17);
            delta3=p(18); r1=p(19); r2=p(20);
9       r3=p(21); rM=p(22); d1=p(23); d2=p(24); d3=p(25);
10 %Maintenance Immunosuppression and ATG
11      emax = p(26); t01 = p(27); t11 = p(28); emin = p(29)
            ;
12      amax = p(30); t02 = p(31); t12 = p(32); amid = p(33)
            ; amin = p(34);
13      eM = emax + (emin-emax)/(t11-t01)*(t-t01)*heaviside(
            t-t01) + (emin - (emax + (emin-emax)/(t11-t01)*(t
            -t01)))*heaviside(t-t11);
14      eA = amax-(amax-amin)/t02*t + (amin+(amid-amin)/(t12
            -t02)*(t-t02)-(amax-(amax-amin)/t02*t)).*
            heaviside(t-t02) + ...
15          (amid - (amin+(amid-amin)/(t12-t02)*(t-t02))).*
                heaviside(t-t12);
```

```
%Rituximab
    eR = interp1(q(:,1),q(:,2),t) + heaviside(t-q(end,1)).*(q(end,2)- interp1(q(:,1),q(:,2),t));
%State variables
    E=x(1); Bn=x(2); Bg=x(3); Bd=x(4); Bm=x(5); Bl=x(6); T1=x(7); T2=x(8); T3=x(9);
%%ODEs
    dx=zeros(9,1);
    dx(1)=n*deltaL*Bl-deltaE*E;%EBV
    dx(2)=(1-eR)*lambdaN-muE*E*Bn-deltaN*Bn;%Naive B cells
    dx(3)=(1-eR)*(1-beta*(1-eA))*muE*E*Bn+(rG-omegaG-deltaG)*Bg-delta1*T1*Bg;%Growth B cells *(1-eA)
    dx(4)=(1-eR)*omegaG*Bg+(rD-deltaD-omegaD)*Bd-delta2*T2*Bd;%GC B cells
    dx(5)=(1-eR)*omegaD*Bd+(rM-omegaM-deltaM)*Bm;%Memory B cells
    dx(6)=(1-eR)*omegaM*Bm-deltaL*Bl-delta3*T3*Bl;%Lytic B cells
    dx(7)=(1-eM)*r1*T1*Bg-d1*T1-(1-eA)*T1;%CTL response to Bg
    dx(8)=(1-eM)*r2*T2*Bd-d2*T2-(1-eA)*T2;%CTL response to Bd
    dx(9)=(1-eM)*r3*T3*Bl-d3*T3-(1-eA)*T3;%CTL response to Bl
```

B.2.4 Maintenance immunosuppression and basiliximab

```
% PTLD project
% ODE file for EBV
% Created by: Michael Akinwumi
% Last modified: Jan 31, 2017
function [dx] = maintenanceBasiliximab(t,x,p)
%Parameters
    rG=p(1); omegaG=p(2); rD=p(3); omegaM = p(4); deltaL=p(5); n=p(6); deltaE=p(7); lambdaN=p(8); beta=p(9); muE=p(10);
    deltaN=p(11); deltaG=p(12); delta1=p(13); deltaD=p(14); omegaD=p(15); delta2=p(16); deltaM=p(17); delta3=p(18); r1=p(19); r2=p(20);
    r3=p(21); rM=p(22); d1=p(23); d2=p(24); d3=p(25);
%Maintenance Immunosuppression and ATG
```

```
11      emax = p(26); t01 = p(27); t11 = p(28); emin = p(29)
            ;
12      bmax = p(30); t02 = p(31); t12 = p(32); bmin = p(33)
            ;
13      eM = emax + (emin-emax)/(t11-t01)*(t-t01)*heaviside(
            t-t01) + (emin - (emax + (emin-emax)/(t11-t01)*(t
            -t01)))*heaviside(t-t11);
14      eB = bmin + (bmax-bmin)/(t12-t02)*(t-t02)*heaviside(
            t-t02) + (bmax - (bmin + (bmax-bmin)/(t12-t02)*(t
            -t02)))*heaviside(t-t12);
15  %State variables
16      E=x(1); Bn=x(2); Bg=x(3); Bd=x(4); Bm=x(5); Bl=x(6);
             T1=x(7); T2=x(8); T3=x(9);
17  %%ODEs
18      dx=zeros(9,1);
19      dx(1)=n*deltaL*Bl-deltaE*E;%EBV
20      dx(2)=lambdaN-muE*E*Bn-deltaN*Bn;%Naive B cells
21      dx(3)=(1-beta)*muE*E*Bn+(rG-omegaG-deltaG)*Bg-delta1
            *T1*Bg;%Growth B cells
22      dx(4)=omegaG*Bg+(rD-deltaD-omegaD)*Bd-delta2*T2*Bd;%
            GC B cells
23      dx(5)=omegaD*Bd+(rM-omegaM-deltaM)*Bm;%Memory B
            cells
24      dx(6)=omegaM*Bm-deltaL*Bl-delta3*T3*Bl;%Lytic B
            cells
25      dx(7)=(eB-1)*(1-eM)*r1*T1*Bg-d1*T1;%CTL response to
            Bg
26      dx(8)=(eB-1)*(1-eM)*r2*T2*Bd-d2*T2;%CTL response to
            Bd
27      dx(9)=(eB-1)*(1-eM)*r3*T3*Bl-d3*T3;%CTL response to
            Bl
```

B.2.5 Maintenance immunosuppression, basiliximab and valganciclovir

```
1  % PTLD project
2  % ODE file for EBV
3  % Created by: Michael Akinwumi
4  % Last modified: Jan 31, 2017
5  function [dx] = maintenanceBasiliximabAntiviral(t,x,p)
6  %Parameters
```

```
7       rG=p(1); omegaG=p(2); rD=p(3); omegaM = p(4); deltaL
            =p(5); n=p(6); deltaE=p(7); lambdaN=p(8); beta=p
            (9); muE=p(10);
8       deltaN=p(11); deltaG=p(12); delta1=p(13); deltaD=p
            (14); omegaD=p(15); delta2=p(16); deltaM=p(17);
            delta3=p(18); r1=p(19); r2=p(20);
9       r3=p(21); rM=p(22); d1=p(23); d2=p(24); d3=p(25);
10  %Maintenance Immunosuppression and ATG
11      emax = p(26); t01 = p(27); t11 = p(28); emin = p(29)
            ;
12      bmax = p(30); t02 = p(31); t12 = p(32); bmin = p(33)
            ;
13      eM = emax + (emin-emax)/(t11-t01)*(t-t01)*heaviside(
            t-t01) + (emin - (emax + (emin-emax)/(t11-t01)*(t
            -t01)))*heaviside(t-t11);
14      eB = bmin + (bmax-bmin)/(t12-t02)*(t-t02)*heaviside(
            t-t02) + (bmax - (bmin + (bmax-bmin)/(t12-t02)*(t
            -t02)))*heaviside(t-t12);
15  %Valganciclovir
16      DV = p(34); VV = p(35); ka = p(36); kel = p(37);
            tauV = p(38); ICV = p(39); epV = p(40); tstart =
            p(41); tend = p(42);
17      nV = heaviside(t-tstart)*(1 + floor((t-tstart)/tauV)
            );
18      CV = DV/VV*ka/(ka-kel)*((1-exp(-nV*kel*tauV))/(1-exp
            (-kel*tauV))*exp(-kel*mod(t,tauV)) - (1-exp(-nV*
            ka*tauV))/(1-exp(-ka*tauV))*exp(-ka*mod(t,tauV)))
            ;
19      eV = epV*CV/(CV + ICV)*heaviside(t-(tstart+2)) - epV
            *CV/(CV + ICV)*heaviside(t-tend);
20  %State variables
21      E=x(1); Bn=x(2); Bg=x(3); Bd=x(4); Bm=x(5); Bl=x(6);
             T1=x(7); T2=x(8); T3=x(9);
22  %%ODEs
23      dx=zeros(9,1);
24      dx(1)=(1-eV/.7)*n*deltaL*Bl-deltaE*E;%EBV
25      dx(2)=lambdaN-muE*E*Bn-deltaN*Bn;%Naive B cells
26      dx(3)=(1-beta)*muE*E*Bn+(rG-omegaG-deltaG)*Bg-delta1
            *T1*Bg;%Growth B cells
27      dx(4)=omegaG*Bg+(rD-deltaD-omegaD)*Bd-delta2*T2*Bd;%
            GC B cells
```

```
28      dx(5)=omegaD*Bd+(rM-omegaM-deltaM)*Bm;%Memory B
            cells
29      dx(6)=omegaM*Bm-deltaL*Bl-delta3*T3*Bl;%Lytic B
            cells
30      dx(7)=(eB-1)*(1-eM)*r1*T1*Bg-d1*T1;%CTL response to
            Bg
31      dx(8)=(eB-1)*(1-eM)*r2*T2*Bd-d2*T2;%CTL response to
            Bd
32      dx(9)=(eB-1)*(1-eM)*r3*T3*Bl-d3*T3;%CTL response to
            Bl
```

B.2.6 Maintenance immunosuppression, basiliximab and rituximab

```
1  % PTLD project
2  % ODE file for EBV
3  % Created by: Michael Akinwumi
4  % Last modified: Jan 31, 2017
5  function [dx] = maintenanceBasiliximabRituximab(t,x,p)
6  %Parameters
7       rG=p(1); omegaG=p(2); rD=p(3); omegaM = p(4); deltaL
            =p(5); n=p(6); deltaE=p(7); lambdaN=p(8); beta=p
            (9); muE=p(10);
8       deltaN=p(11); deltaG=p(12); delta1=p(13); deltaD=p
            (14); omegaD=p(15); delta2=p(16); deltaM=p(17);
            delta3=p(18); r1=p(19); r2=p(20);
9       r3=p(21); rM=p(22); d1=p(23); d2=p(24); d3=p(25);
10 %Maintenance Immunosuppression and ATG
11      emax = p(26); t01 = p(27); t11 = p(28); emin = p(29)
            ;
12      bmax = p(30); t02 = p(31); t12 = p(32); bmin = p(33)
            ;
13      eM = emax + (emin-emax)/(t11-t01)*(t-t01)*heaviside(
            t-t01) + (emin - (emax + (emin-emax)/(t11-t01)*(t
            -t01)))*heaviside(t-t11);
14      eB = bmin + (bmax-bmin)/(t12-t02)*(t-t02)*heaviside(
            t-t02) + (bmax - (bmin + (bmax-bmin)/(t12-t02)*(t
            -t02)))*heaviside(t-t12);
15 %Rituximab
16      eR = interp1(q(:,1),q(:,2),t) + heaviside(t-q(end,1)
            )*(q(end,2)- interp1(q(:,1),q(:,2),t));
17 %State variables
```

```
18      E=x(1); Bn=x(2); Bg=x(3); Bd=x(4); Bm=x(5); Bl=x(6);
            T1=x(7); T2=x(8); T3=x(9);
19  %%ODEs
20      dx=zeros(9,1);
21      dx(1)=n*deltaL*Bl-deltaE*E;%EBV
22      dx(2)=(1-eR)*lambdaN-muE*E*Bn-deltaN*Bn;%Naive B
            cells
23      dx(3)=(1-eR)*(1-beta)*muE*E*Bn+(rG-omegaG-deltaG)*Bg
            -delta1*T1*Bg;%Growth B cells
24      dx(4)=(1-eR)*omegaG*Bg+(rD-deltaD-omegaD)*Bd-delta2*
            T2*Bd;%GC B cells
25      dx(5)=(1-eR)*omegaD*Bd+(rM-omegaM-deltaM)*Bm;%Memory
             B cells
26      dx(6)=(1-eR)*omegaM*Bm-deltaL*Bl-delta3*T3*Bl;%Lytic
             B cells
27      dx(7)=(eB-1)*(1-eM)*r1*T1*Bg-d1*T1;%CTL response to
            Bg
28      dx(8)=(eB-1)*(1-eM)*r2*T2*Bd-d2*T2;%CTL response to
            Bd
29      dx(9)=(eB-1)*(1-eM)*r3*T3*Bl-d3*T3;%CTL response to
            Bl
```